[redacted]

RESEARCH MEMORANDUM

WIND-TUNNEL INVESTIGATION AT HIGH SUBSONIC SPEEDS OF SOME EFFECTS OF FUSELAGE CROSS-SECTION SHAPE AND WING HEIGHT ON THE STATIC LONGITUDINAL AND LATERAL STABILITY CHARACTERISTICS OF A MODEL HAVING A 45° SWEPT WING

By Thomas J. King, Jr.

Langley Aeronautical Laboratory
Langley Field, Va.

CLASSIFIED DOCUMENT

NATIONAL ADVISORY COMMITTEE
FOR AERONAUTICS

WASHINGTON

February 3, 1956

[redacted]

NACA RM L55J25

NATIONAL ADVISORY COMMITTEE FOR AERONAUTICS

RESEARCH MEMORANDUM

WIND-TUNNEL INVESTIGATION AT HIGH SUBSONIC SPEEDS OF SOME EFFECTS OF FUSELAGE CROSS-SECTION SHAPE AND WING HEIGHT ON THE STATIC LONGITUDINAL AND LATERAL STABILITY CHARACTERISTICS OF A MODEL HAVING A 45° SWEPT WING

By Thomas J. King, Jr.

SUMMARY

An investigation was conducted in the Langley high-speed 7- by 10-foot tunnel at Mach numbers from 0.80 to 0.92 to determine some effects of fuselage shape on the aerodynamic characteristics of a model having low and high wing arrangements. The results showed that when the cross section of a fuselage was changed from a circular to an essentially square shape, the location of the aerodynamic center for the wing-body combination was moved forward. With the tail on, the high-wing model with the circular fuselage cross section had the most favorable variation of pitching moment over the lift-coefficient range.

The directional stability was greatest for a low-wing configuration with a fuselage having a half-circular cross section on top and a half-square cross section below. The square-fuselage configurations became directionally unstable at an angle of attack of about 12° with the wing in either high or low position; whereas the high-wing—circular-fuselage model became directionally unstable at an angle of attack of about 17° and the low-wing—circular-fuselage model remained stable through the test angle-of-attack range.

Fuselage cross section had little effect at low angles of attack on the effective dihedral derivative; but, at high angles of attack, the square fuselage provided considerably more effective dihedral than the circular fuselage.

INTRODUCTION

The National Advisory Committee for Aeronautics is conducting wind-tunnel investigations to determine the aerodynamic characteristics of airplane models with various arrangements of the component parts. Some results of investigations at low speed have been reported in reference 1, at high subsonic speeds in reference 2, and at supersonic speeds in references 3 and 4.

This paper presents results which show some effects of fuselage cross-section shape and wing height on the longitudinal aerodynamic characteristics and static lateral derivatives of a model having a 45° swept wing of aspect ratio 4, taper ratio 0.3, and with an NACA 65A006 airfoil section in combination with a fuselage of fineness ratio 10.95. The test Mach number range was from 0.80 to 0.92; the corresponding Reynolds numbers (based on wing mean aerodynamic chord) varied from 2.5×10^6 to 3.0×10^6.

COEFFICIENTS AND SYMBOLS

The force and moment coefficients are presented about the stability axes system shown in figure 1. The pitching-moment and yawing-moment axes intersect on the fuselage center line and are located 31.22 inches from the fuselage nose (longitudinal location of quarter-chord point of wing mean aerodynamic chord).

C_L lift coefficient, $\frac{\text{Lift}}{qS}$

C_D drag coefficient, $\frac{\text{Drag}}{qS}$

C_m pitching-moment coefficient, $\frac{\text{Pitching moment}}{qS\bar{c}}$

C_Y side-force coefficient, $\frac{\text{Side force}}{qS}$

C_n yawing-moment coefficient, $\frac{\text{Yawing moment}}{qSb}$

C_l rolling-moment coefficient, $\frac{\text{Rolling moment}}{qSb}$

q dynamic pressure, $\frac{\rho V^2}{2}$, lb/sq ft

[redacted]

V	free-stream velocity, ft/sec
ρ	mass density of air, slugs/cu ft
S	wing area, 2.25 sq ft
b	wing span, 3.00 ft
$\bar{c}$	wing mean aerodynamic chord, $\frac{2}{S}\int_0^{b/2} c^2 dy$, 0.822 ft
$\bar{c}_H$	horizontal-tail mean aerodynamic chord, 0.388 ft
$\bar{c}_V$	vertical-tail mean aerodynamic chord, 0.757 ft
c	local chord parallel to plane of symmetry, ft
y	spanwise distance from plane of symmetry, ft
M	Mach number
α	angle of attack, deg
β	angle of sideslip, deg

$$C_{m_{C_L}} = \frac{\partial C_m}{\partial C_L}$$

$$C_{Y_\beta} = \frac{\partial C_Y}{\partial \beta}$$

$$C_{n_\beta} = \frac{\partial C_n}{\partial \beta}$$

$$C_{l_\beta} = \frac{\partial C_l}{\partial \beta}$$

[redacted]

MODELS AND APPARATUS

A three-view drawing of the model is presented in figure 2 together with tables of the geometric characteristics of the wing and tail surfaces. Coordinates of the fuselage profile and details of the fuselage cross-section shapes are given in figure 3. The corners of the rectangular-sided cross sections were rounded to a radius equal to 6.4 percent of the section width. The profiles of the fuselages were identical for the three cross-section shapes (see fig. 3) but the half-circular-half-square and square cross-section areas were greater than the circular cross-section area by about 13 percent and 27 percent, respectively. A photograph of the low-wing—square-fuselage model mounted on the sting in the Langley high-speed 7- by 10-foot tunnel is shown in figure 4.

The chord plane of the wing was located on the fuselage 2.00 inches from the plane of the fuselage center line (fig. 2). The fuselage nose and center sections could be rotated 180° about the fuselage longitudinal axis to place the wing in a low or high position. The complete model, consisting of wing and fuselage with or without tail surfaces, was attached to the supporting sting (fig. 4) by a six-component internal strain-gage balance. The model forces and moments were measured by the balance and recorded automatically.

TESTS

The sting-supported model was tested in the Langley high-speed 7- by 10-foot tunnel over a Mach number range from 0.80 to 0.92. The Reynolds number (based on wing mean aerodynamic chord) varied from about 2.5×10^6 to 3.0×10^6. The angle of attack varied from -3° to a maximum of 24°; but as the Mach number was increased, the maximum angle of attack was limited by balance loads or available tunnel power. With the wing in the low position, tests were made with the circular, half-circular-half-square, and square fuselage shapes. Tests were made on the circular and square fuselage shapes with the wing in the high position. Static longitudinal characteristics were obtained through the angle-of-attack range at $\beta = 0°$. During the longitudinal tests of the circular fuselage, only the horizontal tail was removed. In the rest of the tail-off tests, including the lateral parameter tests, the horizontal tail as well as the vertical tail was removed. Static lateral characteristics were obtained through the angle-of-attack range at nominal sideslip angles of ±4°. The static lateral stability parameters were computed at each angle of attack by taking the algebraic differences between C_n, C_Y, and C_l at the two angles of sideslip (±4°). These values were then

divided by the difference in sideslip angle which varied slightly from the nominal value of 8° because of corrections to β due to deflection of the balance and sting under load.

CORRECTIONS

Blocking corrections applied to Mach number and dynamic pressure were determined by the method of reference 5. Jet-boundary corrections determined from reference 6 were applied to the angle of attack and drag. Corrections due to longitudinal pressure gradient were applied to the drag data. No model-support tares have been applied to the results. Drag data have been adjusted to correspond to a pressure at the base of the fuselage equal to free-stream static pressure.

The angles of attack and angles of sideslip have been corrected for deflection of the sting support and balance. No attempt has been made to correct the data for aeroelastic deformation of the model as the corrections are believed to be small. (See ref. 7.)

PRESENTATION OF RESULTS

The results of this investigation are presented in figures listed as follows:

Longitudinal characteristics of:	Figure
Low-wing—circular-fuselage combination	5
High-wing—circular-fuselage combination	6
Low-wing—square-fuselage combination	7
High-wing—square-fuselage combination	8
Variation of $C_{m_{C_L}}$ with Mach number	9
Summary of effects of body shape and wing height on variation of C_m against C_L at M = 0.80	10
Static lateral stability parameters of:	
Low-wing—circular-fuselage combination	11
High-wing—circular-fuselage combination	12
Low-wing—half-circular-half-square-fuselage combination	13
Low-wing—square-fuselage combination	14
High-wing—square-fuselage combination	15

[redacted]

Figure

Comparison of the variation of C_{Y_β}, C_{n_β}, and C_{l_β} with α at M = 0.80 16

Increments of static lateral derivatives due to tail 17

DISCUSSION

Longitudinal Stability Characteristics

Fuselage cross-section shape and wing position had little effect on the variation of lift coefficient with angle of attack (figs. 5(a) to 8(a)). The drag of the square-fuselage configurations near zero lift was, in general, slightly higher than the drag of the circular-fuselage configuration, probably because of the larger volume of the square fuselage.

The slopes of the pitching-moment curves against C_L for circular- and square-fuselage models have been measured at zero lift and are presented in figure 9. In general, the aerodynamic center moved rearward with increasing Mach number for all configurations. The aerodynamic-center location of the circular-fuselage configuration (tail off) was from 1.0 to 2.5 percent of the mean aerodynamic chord more rearward than that of the square-fuselage configuration except at the highest Mach number. The aerodynamic-center location of the circular-fuselage configuration with the tail on was about 2.0 to 3.0 percent of the mean aerodynamic chord more rearward than that of the square-fuselage configuration at all Mach numbers.

In reference 8, it is shown that the shape of the static pitching-moment curve is a primary factor affecting the dynamic pitch-up motions of an airplane. Examination of the pitching-moment curves of figures 5 to 8 indicates that at moderate lift coefficients, regions of decreased stability were present for all configurations investigated. The pitching-moment curves of the circular-fuselage configurations (high and low wing positions) had less severe breaks than those of comparable square-fuselage configurations (fig. 10). The addition of the horizontal tail compensated a large part of the unstable breaks for both fuselage shapes with the wing in the high position; the stabilizing effect of the horizontal tail was not as strong on the low-wing configurations. In general, the complete model with the high wing and circular fuselage had the most favorable variation of pitching moment with lift over the Mach number range investigated.

Lateral Stability Characteristics

Low-wing configurations.- Fuselage cross-section shape had large effects on the lateral stability characteristics of the low-wing models, particularly at angles of attack above about 4°. Comparison curves showing the variation of C_{Y_β}, C_{n_β}, and C_{l_β} with angle of attack at $M = 0.80$ are presented in figure 16. A decrease in the directional stability of the square-fuselage configuration resulted from the decrease in the increment of C_{Y_β} due to the tail. From figure 16 it is seen that the square-fuselage configuration (tail on) became directionally unstable at $\alpha \approx 12^\circ$. The value of C_{n_β} and the increment in C_{n_β} due to the tail at $M = 0.80$ (figs. 16 and 17) were larger for the half-circular-half-square-fuselage than for either the circular- or the square-fuselage configuration. In general, for the three low-wing configurations tested, variation in Mach number from 0.80 to 0.92 produced slight improvements in directional stability characteristics.

In the low-angle-of-attack range, fuselage cross-section shape had little effect on C_{l_β}. For all configurations the variation of C_{l_β} with low and moderate angles of attack increased slightly with increase in Mach number. At angles of attack above approximately 4°, the variation of C_{l_β} with α became markedly nonlinear and behaved in the manner described in reference 9 relating to swept wings. At angles of attack above 10°, ΔC_{l_β} (fig. 17) became positive for the circular- and half-circular-half-square-fuselage configurations but remained negative for the square-fuselage model.

High-wing configurations.- The change in wing position from low to high had little effect on the angle of attack at which the square-fuselage configuration (tail on) became directionally unstable; although, as has been shown in other investigations, changing the wing position from low to high on the circular-fuselage configuration (tail on) resulted in a significant deterioriation in directional stability, particularly at high angles of attack (fig. 16). At low angles of attack, raising the wing produced the usual reduction in ΔC_{n_β} for all configurations. For the high-wing configurations there was little effect of fuselage cross-section shape on the increment in C_{n_β} due to the tail.

At low angles of attack, about the same increase in effective dihedral $\left(-C_{l_\beta}\right)$ resulted from raising the wing from a low to a high position for either the circular- or square-fuselage configurations. At high angles of attack, the square-fuselage model had considerably higher effective dihedral than the circular-fuselage model.

[redacted]

CONCLUSIONS

An investigation was made to determine the aerodynamic characteristics at high subsonic speeds of a wing of aspect ratio 4, taper ratio 0.3, sweep of 45°, and with an NACA 65A006 airfoil section mounted in a low and a high position on fuselages of fineness ratio 10.95 with circular, half-circular-half-square, and square cross-section shapes. The results of this investigation indicate the following conclusions:

1. The configurations with the circular-fuselage cross sections generally had the more rearward aerodynamic centers compared to the configurations with the square fuselage cross sections.

2. The high-wing—circular-fuselage configuration (tail on) had the most favorable pitching-moment variation with lift; however, at moderate lift coefficients, regions of decreased stability were present for all configurations.

3. The square-fuselage complete model became directionally unstable at about an angle of attack of 12° with the wing in either a high or low position; whereas the circular-fuselage model with the low wing remained stable throughout the angle-of-attack range and the high-wing—circular-fuselage model became unstable at about 17° angle of attack. The most favorable directional stability characteristics were obtained for the low-wing model with a fuselage having a half-circular cross section on top and a square cross section below.

4. Fuselage cross section had little effect on the effective dihedral parameter at low angles of attack; but, at high angles of attack, the square fuselage provided considerably more effective dihedral than the circular fuselage.

Langley Aeronautical Laboratory,
National Advisory Committee for Aeronautics,
Langley Field, Va., October 18, 1955.

[redacted]

REFERENCES

1. Letko, William, and Williams, James L.: Experimental Investigation at Low Speed of Effects of Fuselage Cross Section on Static Longitudinal and Lateral Stability Characteristics of Models having 0° and 45° Sweptback Surfaces. NACA TN 3551, 1955.

2. Goodson, Kenneth W., and Becht, Robert E.: Wind-Tunnel Investigation at High Subsonic Speeds of the Stability Characteristics of a Complete Model Having Sweptback-, M-, W-, and Cranked-Wing Plan Forms and Several Horizontal-Tail Locations. NACA RM L54C29, 1954.

3. Spearman, M. Leroy: Investigation of the Aerodynamic Characteristics in Pitch and Sideslip of a 45° Sweptback-Wing Airplane Model With Various Vertical Locations of the Wing and Horizontal Tail - Effect Of Wing Location and Geometric Dihedral for the Wing-Body Combination, M = 2.01. NACA RM L55B18, 1955.

4. Carlson, Harry W., and Gapcynski, John P.: An Experimental Investigation at a Mach Number of 2.01 of the Effects of Body Cross-Section Shape on the Aerodynamic Characteristics of Bodies and Wing-Body Combinations. NACA RM L55E23, 1955.

5. Herriot, John G.: Blockage Correction for Three-Dimensional-Flow Closed-Throat Wind Tunnels, With Consideration of the Effect of Compressibility. NACA Rep. 995, 1950. (Supersedes NACA RM A7B28.)

6. Gillis, Clarence L., Polhamus, Edward C., and Gray, Joseph L., Jr.: Charts for Determining Jet-Boundary Corrections for Complete Models in 7- by 10-Foot Closed Rectangular Wind Tunnels. NACA WR L-123, 1945. (Formerly NACA ARR L5G31.)

7. King, Thomas J., Jr., and Pasteur, Thomas B., Jr.: Wind-Tunnel Investigation of the Aerodynamic Characteristics in Pitch of Wing-Fuselage Combinations at High Subsonic Speeds - Taper-Ratio Series. NACA RM L53E20, 1953.

8. Campbell, George S., and Weil, Joseph: The Interpretation of Nonlinear Pitching Moments in Relation to the Pitch-Up Problem. NACA RM L53I02, 1953.

9. Polhamus, Edward C., and Sleeman, William C., Jr.: The Rolling Moment Due to Sideslip of Swept Wings at Subsonic and Transonic Speeds. NACA RM L54L01, 1955.

[redacted]

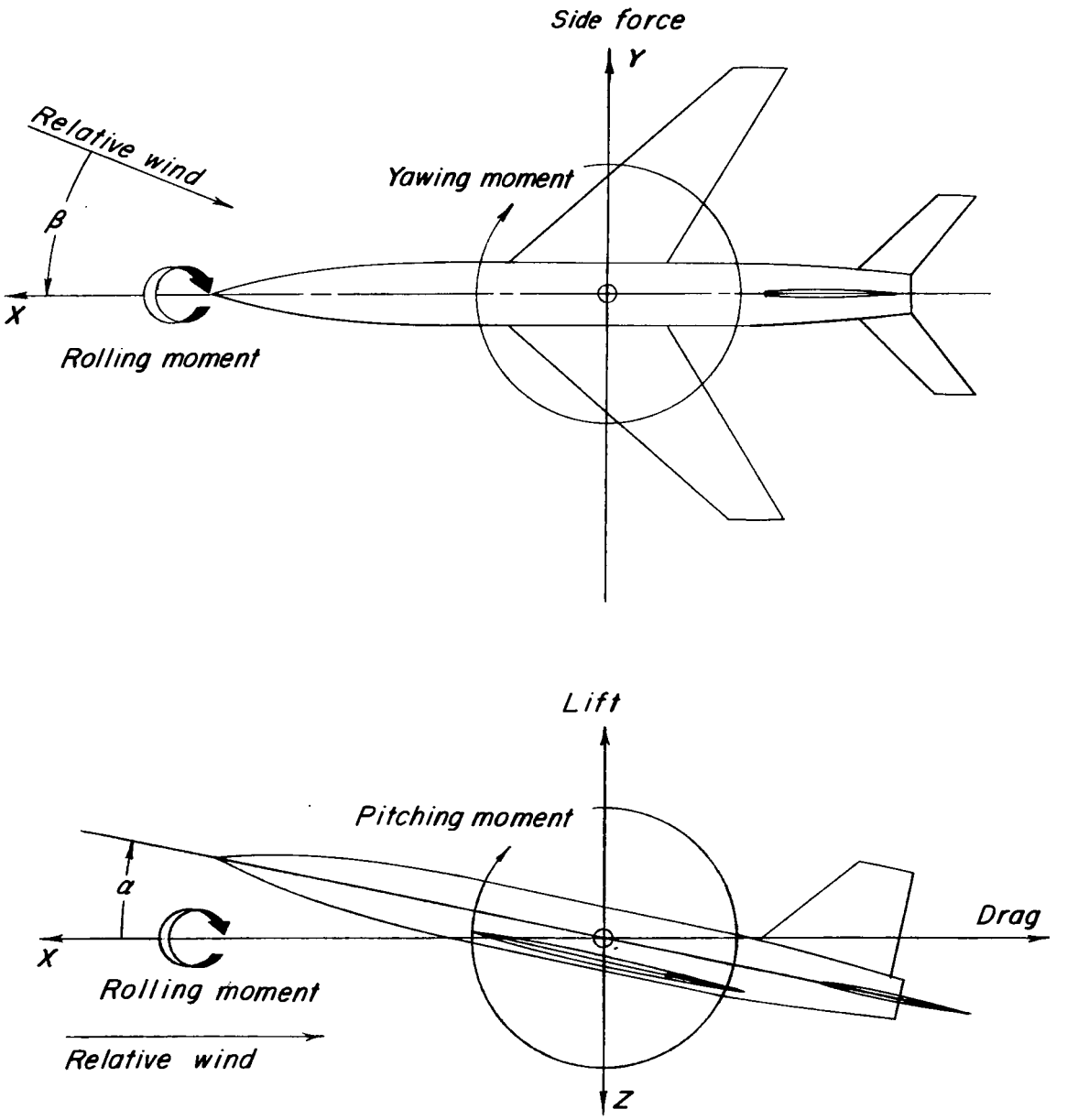

Figure 1.- Stability system of axes. Positive direction of forces, moments, and angles are indicated by arrows.

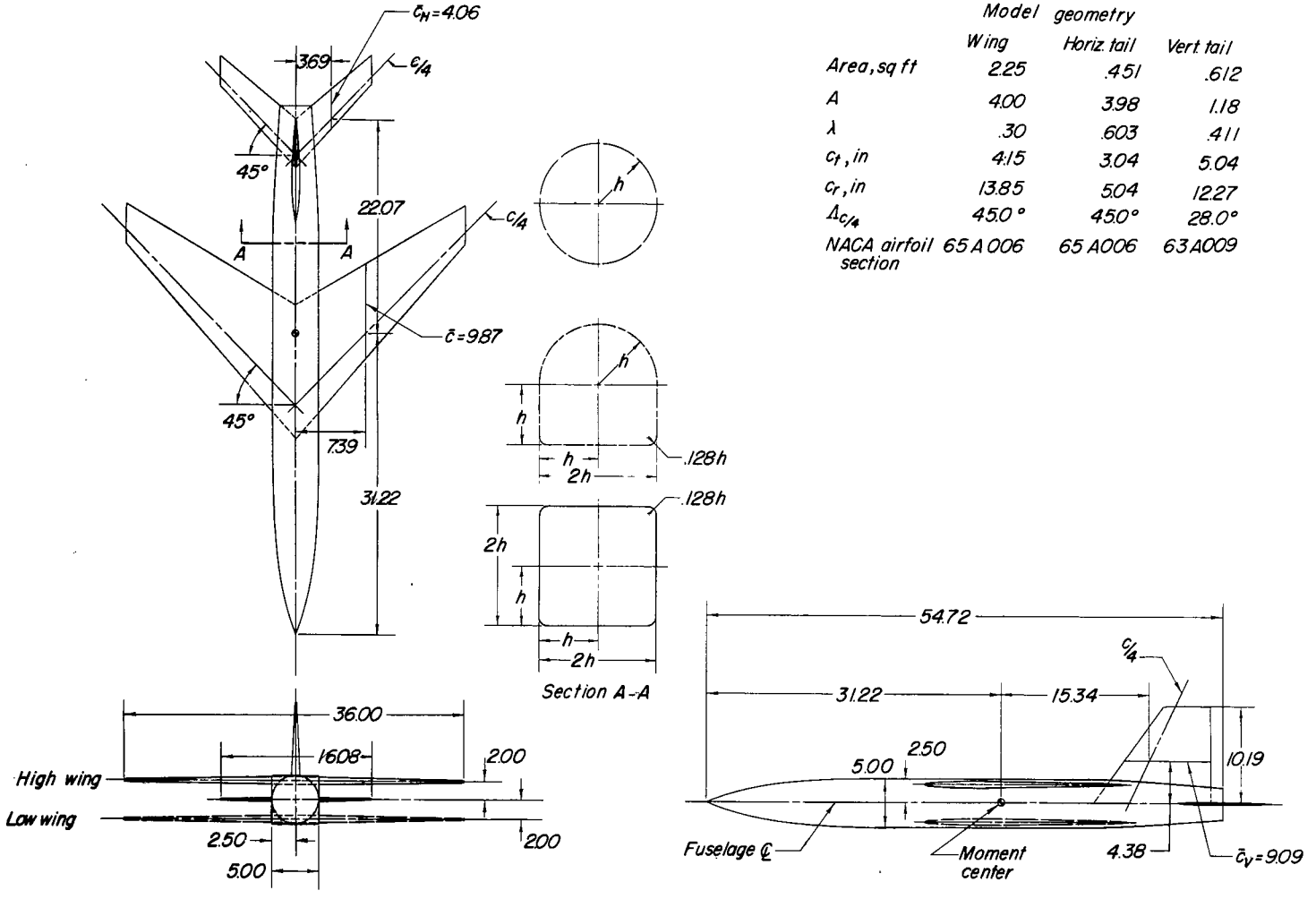

Model geometry

	Wing	Horiz. tail	Vert. tail
Area, sq ft	2.25	.451	.612
A	4.00	3.98	1.18
λ	.30	.603	.411
c_t, in	4.15	3.04	5.04
c_r, in	13.85	5.04	12.27
$\Lambda_{c/4}$	45.0°	45.0°	28.0°
NACA airfoil section	65A006	65A006	63A009

Figure 2.- Three-view drawing of model with circular, square, and half-circular-half-square fuselage cross-section shapes. All dimensions are in inches.

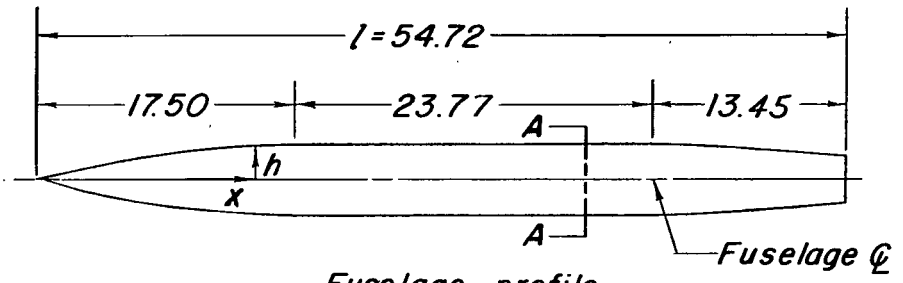

Fuselage profile

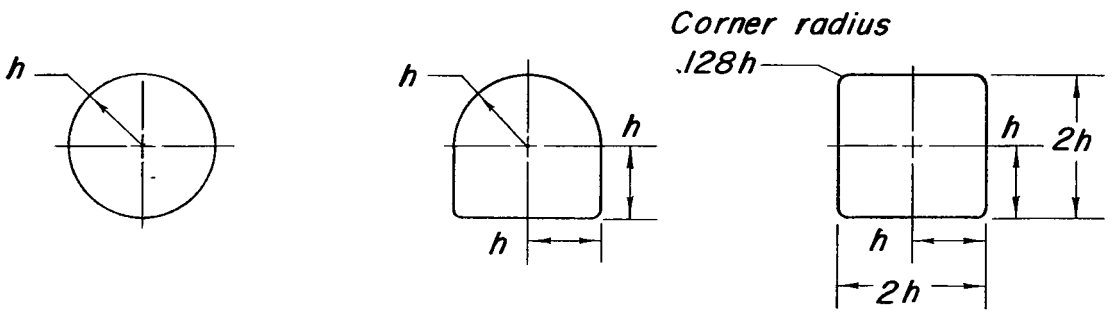

Section A-A Section A-A Section A-A

Fuselage cross sections

Profile Coordinates

x	h
0.	0
2.00	.53
4.00	1.00
6.00	1.44
8.00	1.80
10.00	2.07
12.00	2.30
14.00	2.42
16.00	2.47
17.50	2.50
41.27	2.50
43.27	2.42
45.27	2.35
47.27	2.25
48.30	2.14
54.72	1.65

Figure 3.- Fuselage dimensions showing profile and cross sections' geometry. All dimensions are in inches.

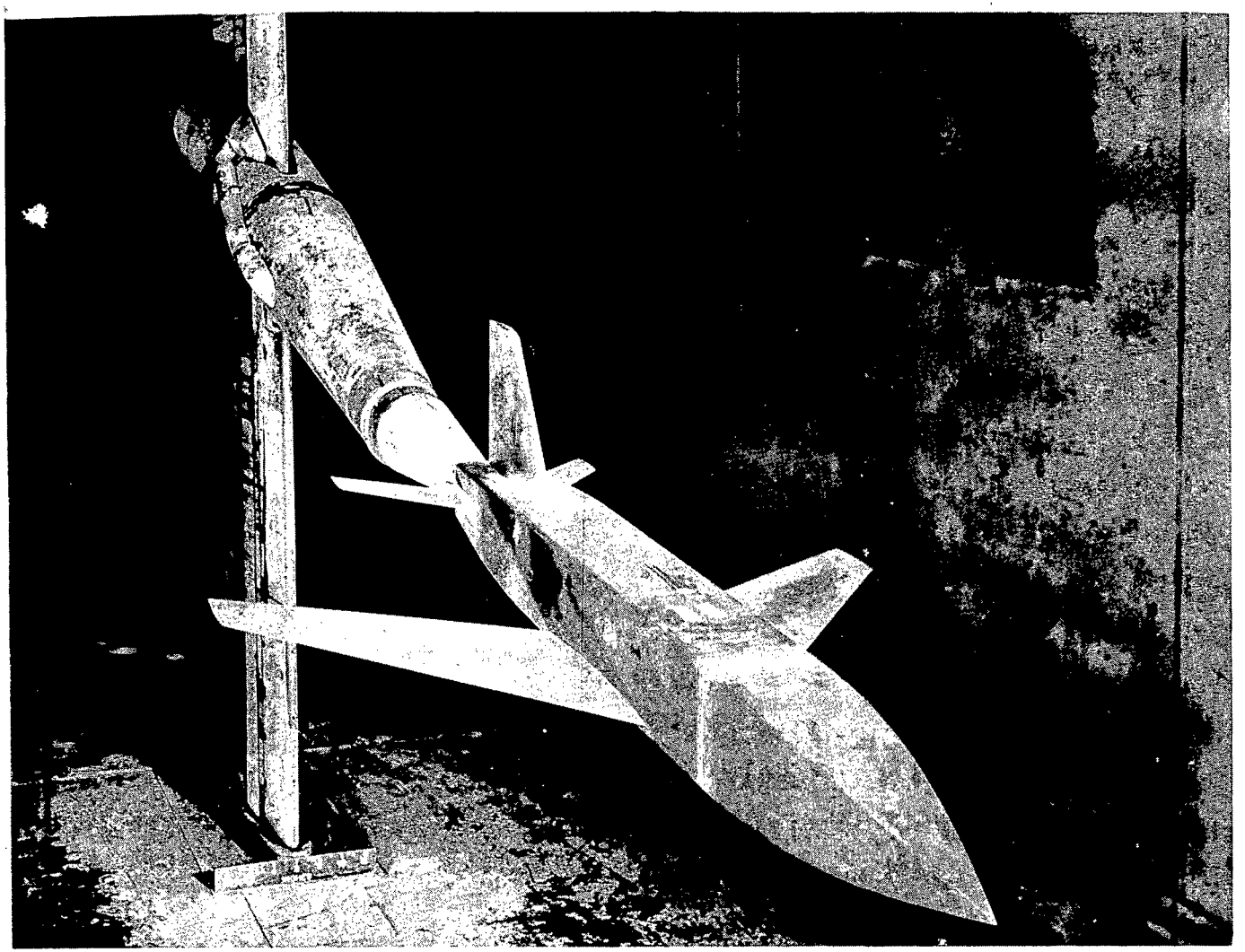

L-86919

Figure 4.- Photograph of model mounted in the Langley high-speed 7- by 10-foot tunnel.

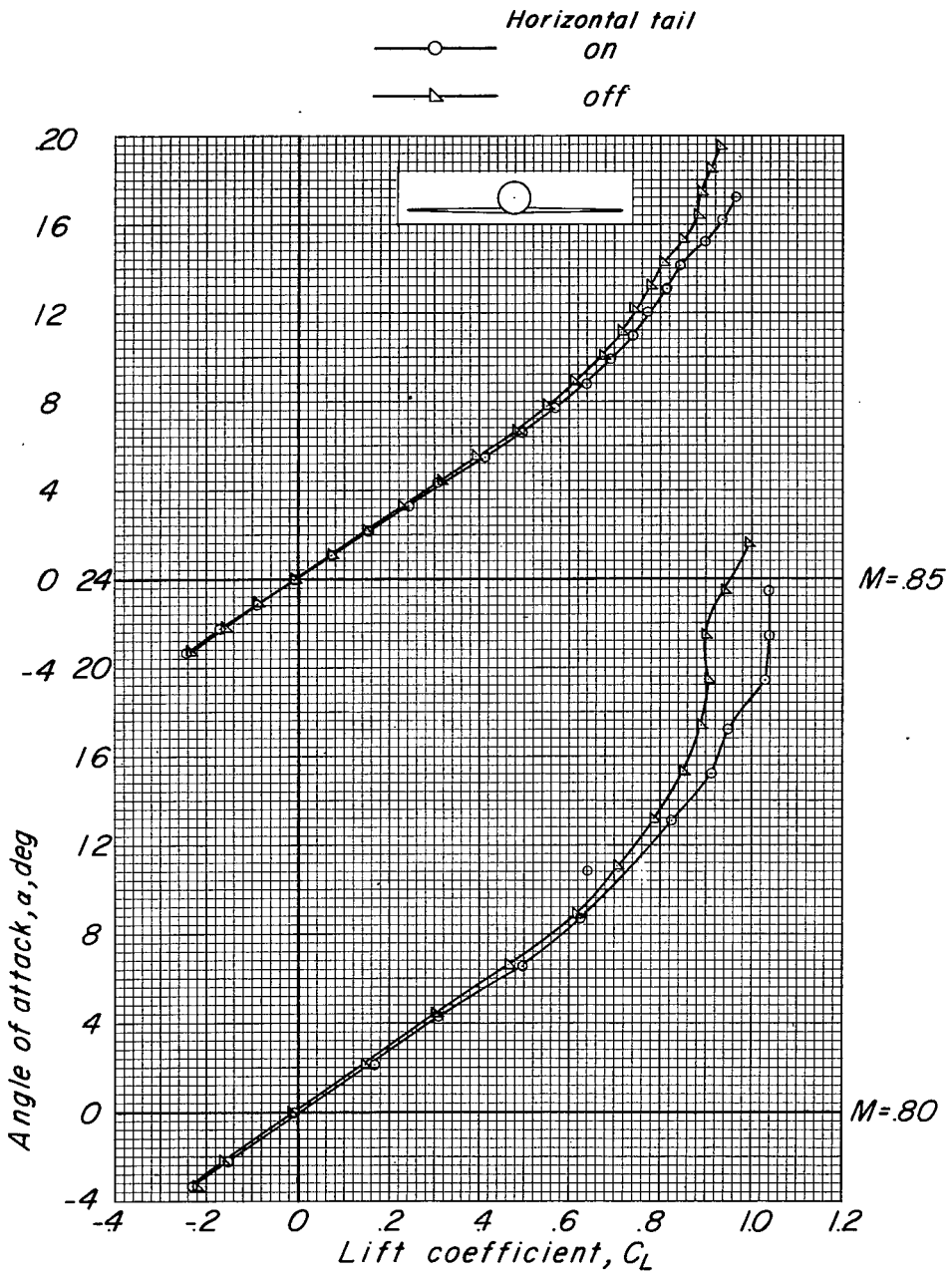

(a) α against C_L.

Figure 5.- Longitudinal characteristics of model with low wing, vertical tail, and circular fuselage.

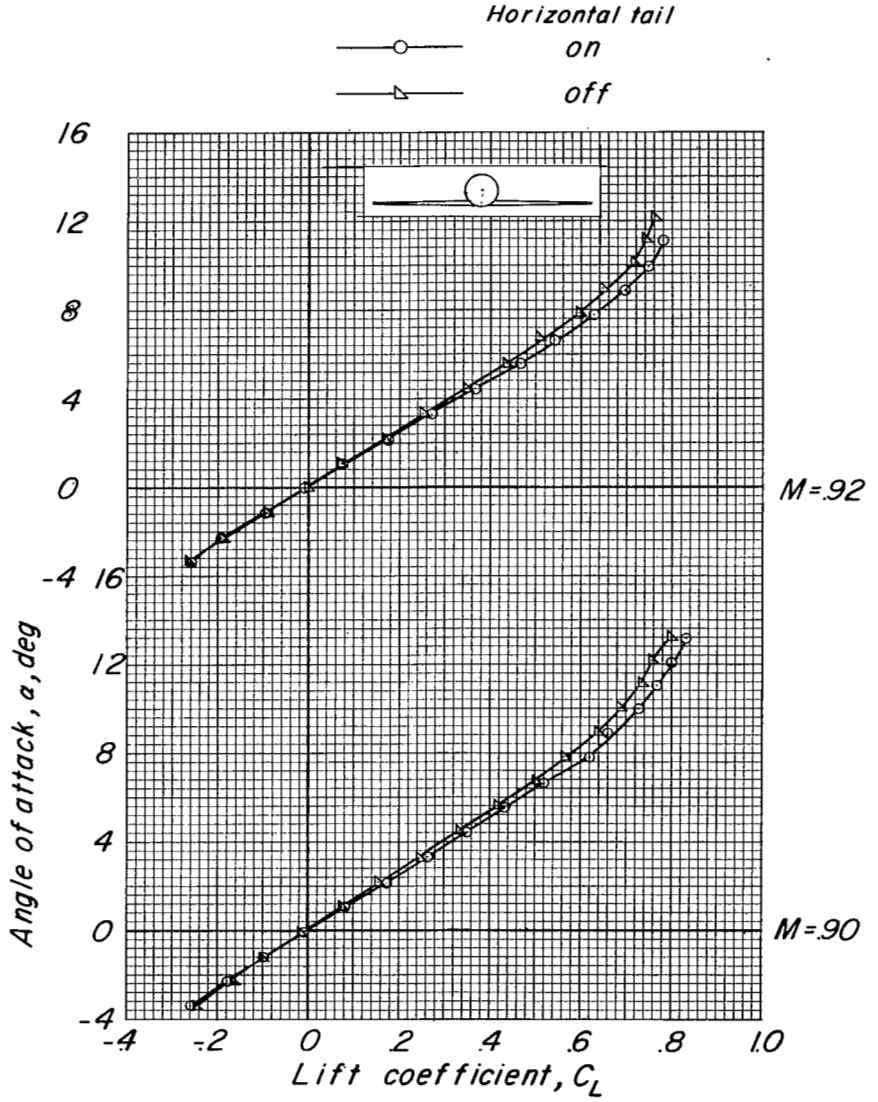

(a) Concluded.

Figure 5.- Continued.

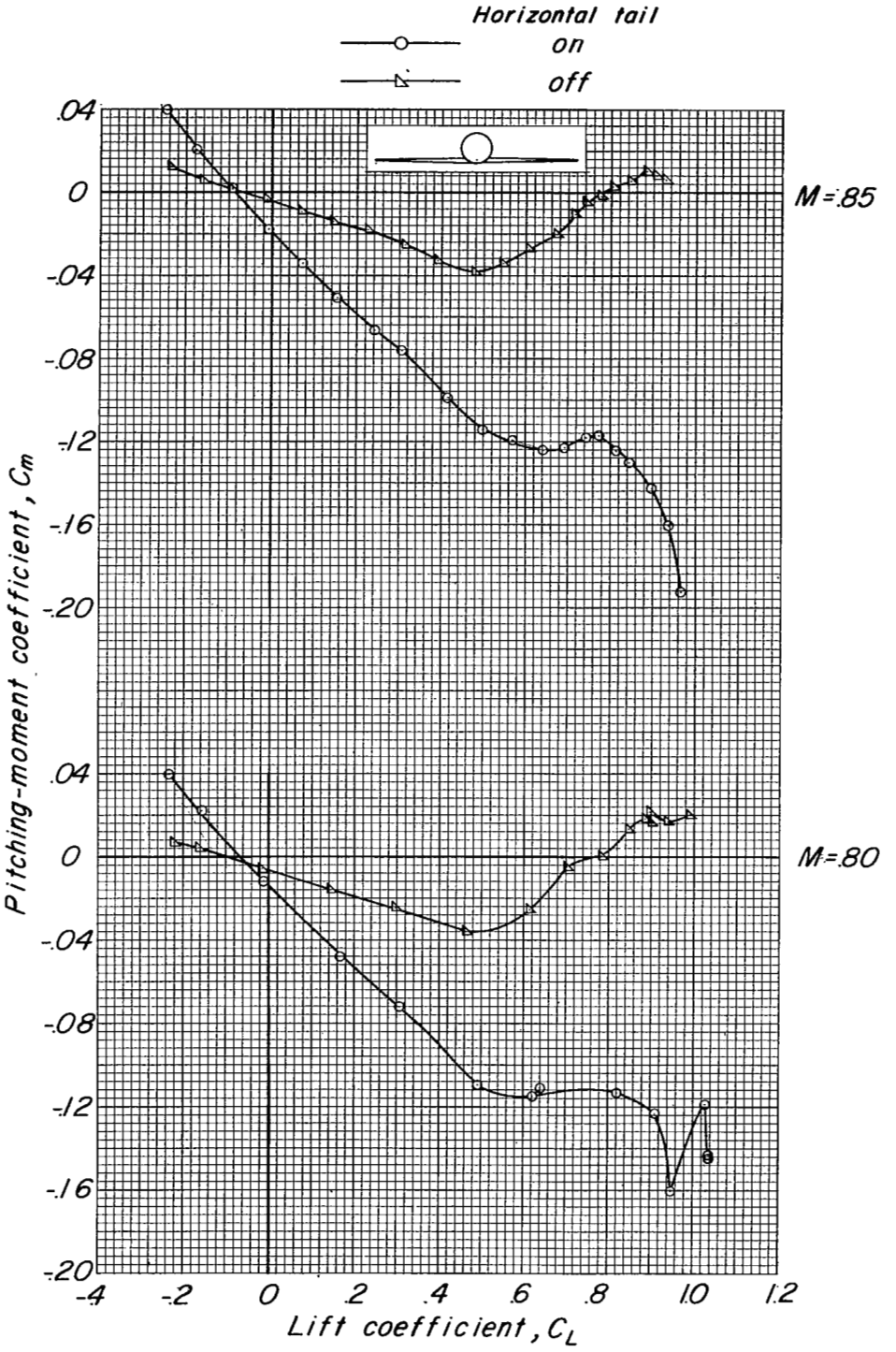

(b) C_m against C_L.

Figure 5.- Continued.

[redacted]

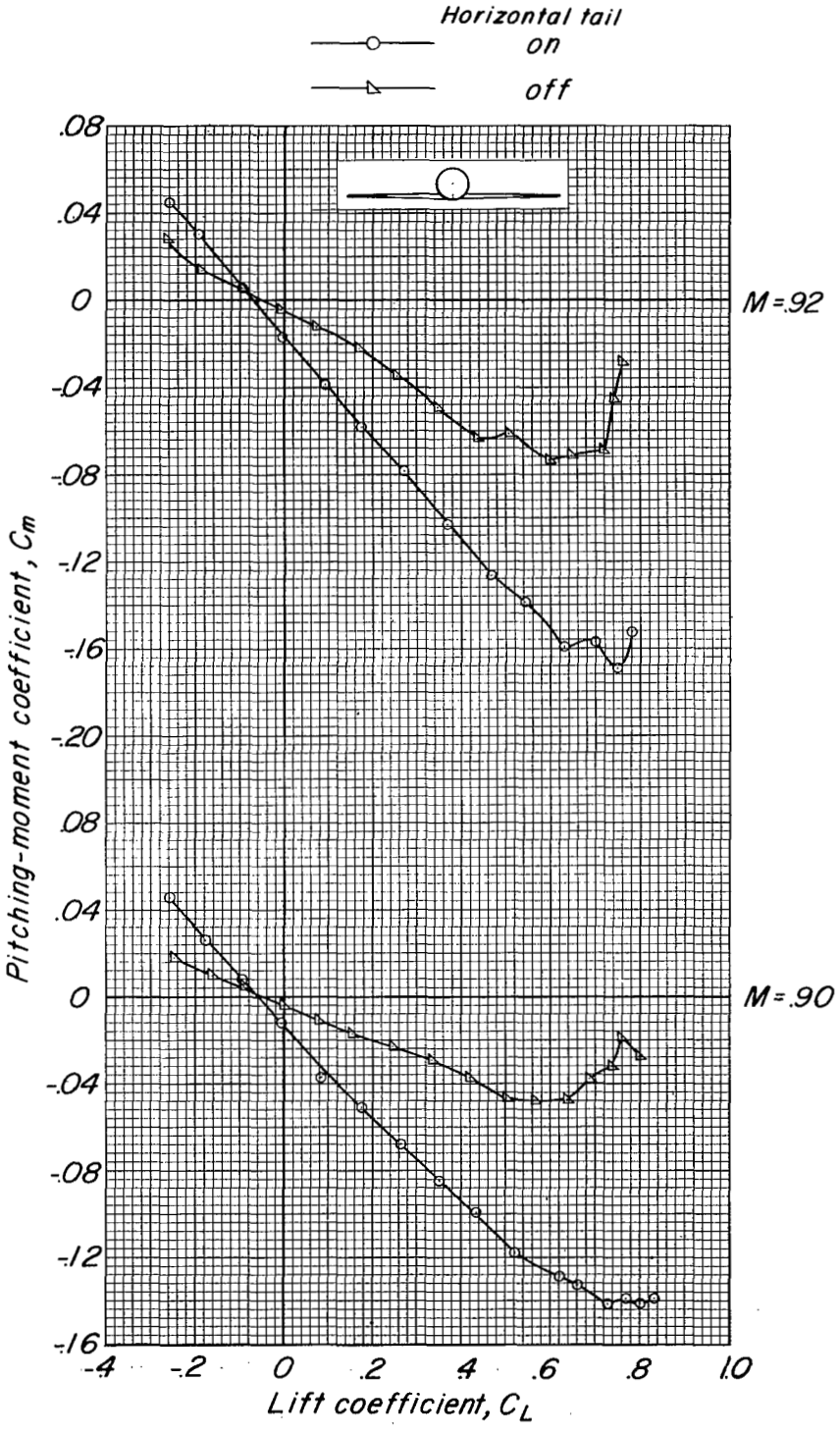

(b) Concluded.

Figure 5.- Continued.

[redacted]

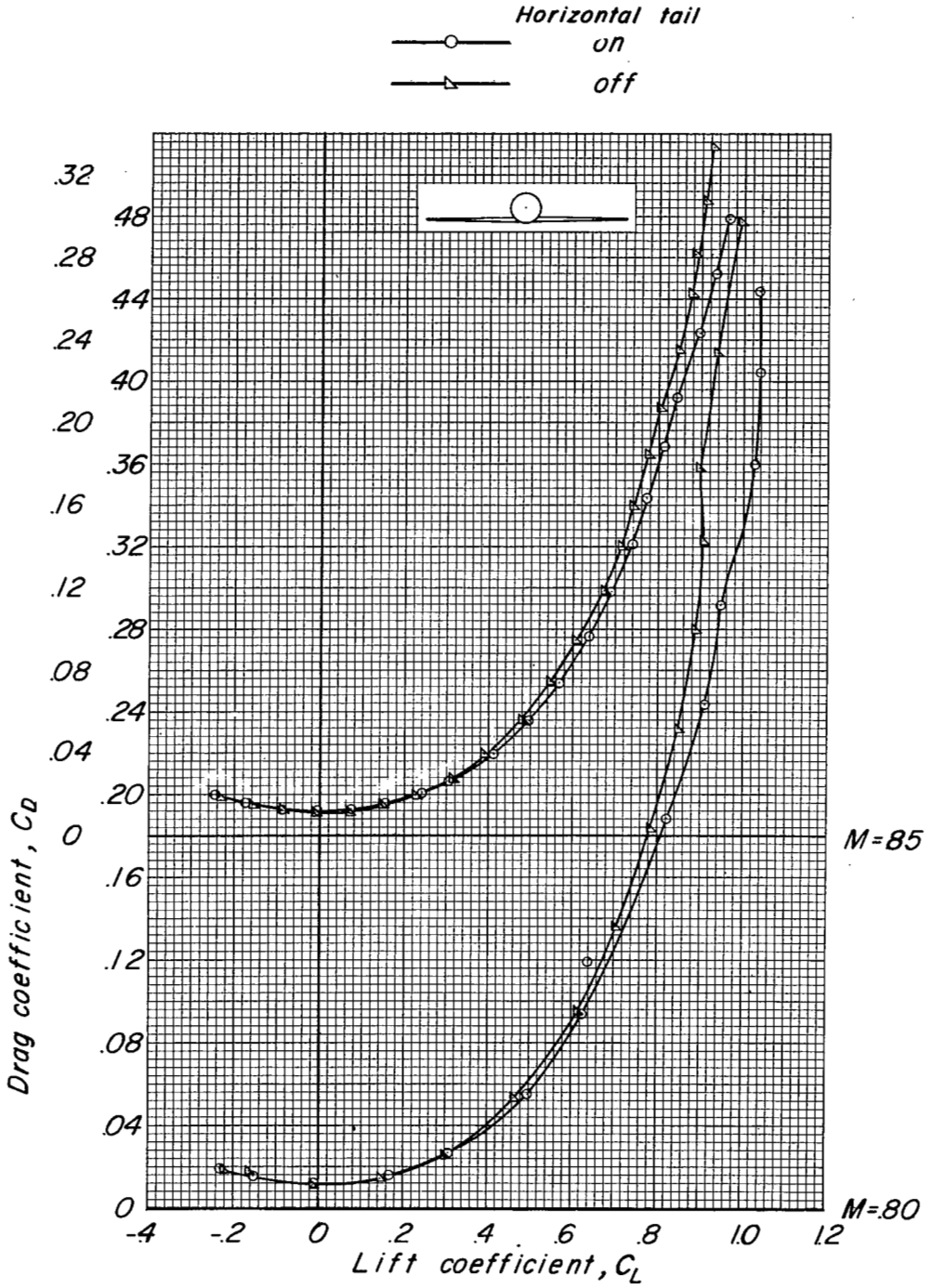

(c) C_D against C_L.

Figure 5.- Continued.

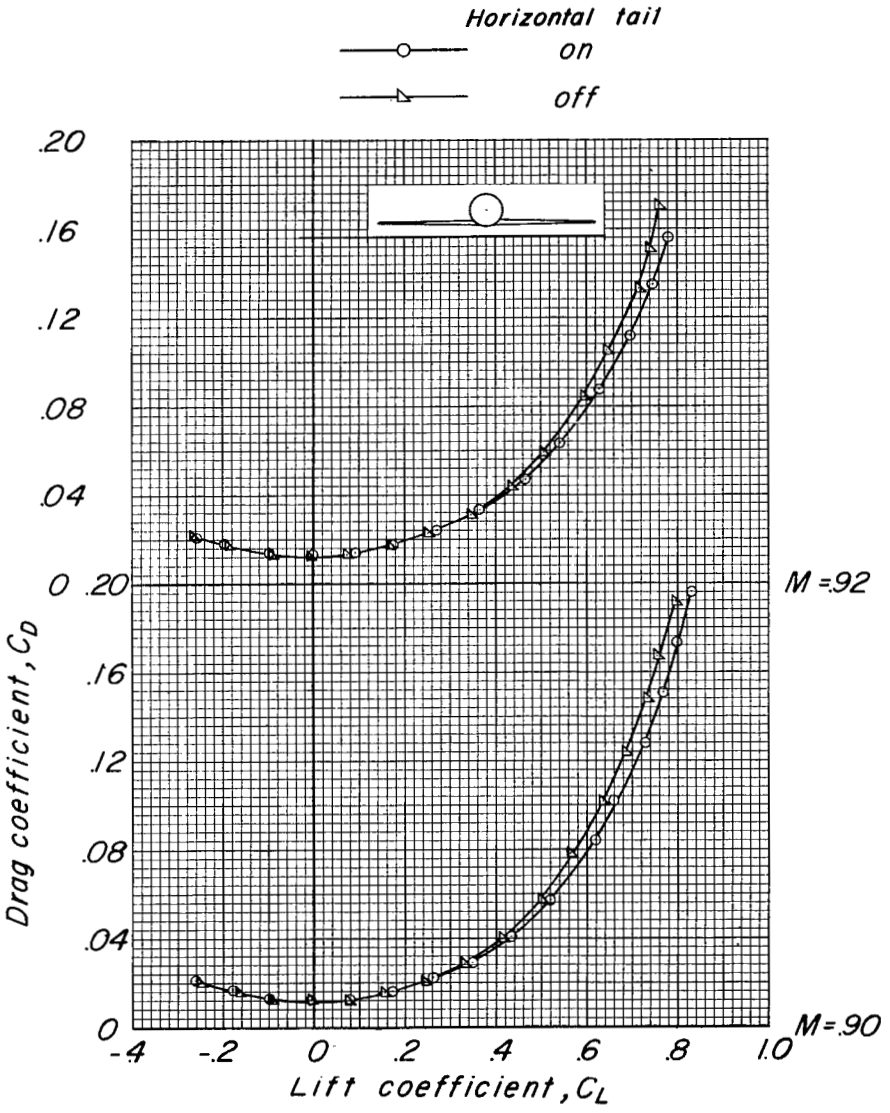

(c) Concluded.

Figure 5.- Concluded.

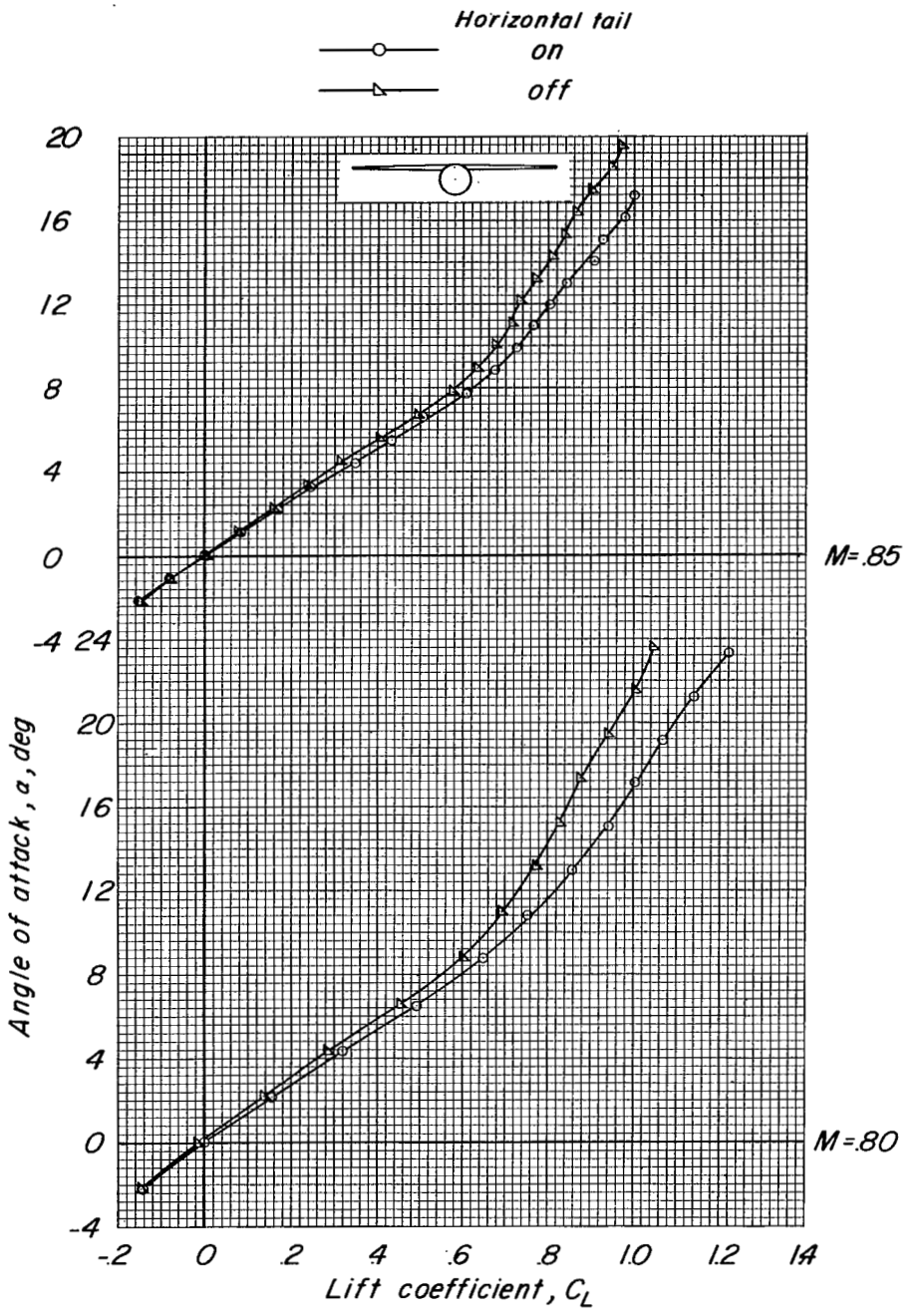

(a) α against C_L.

Figure 6.- Longitudinal characteristics of model with high wing, vertical tail, and circular fuselage.

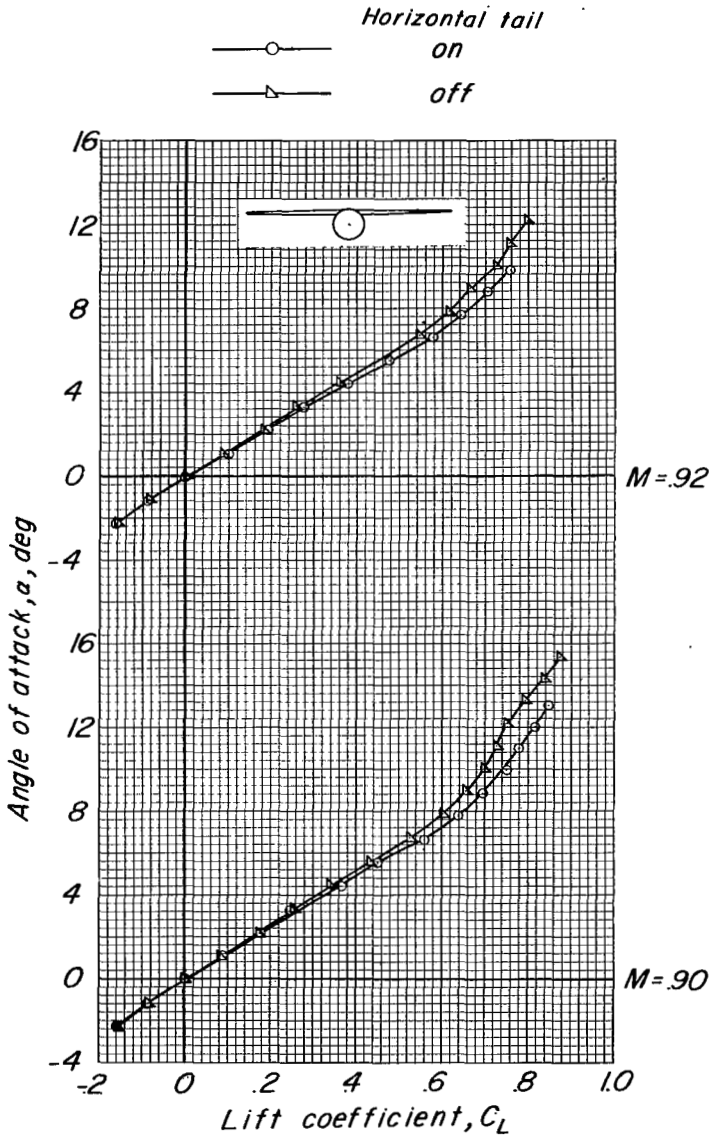

(a) Concluded.

Figure 6.- Continued.

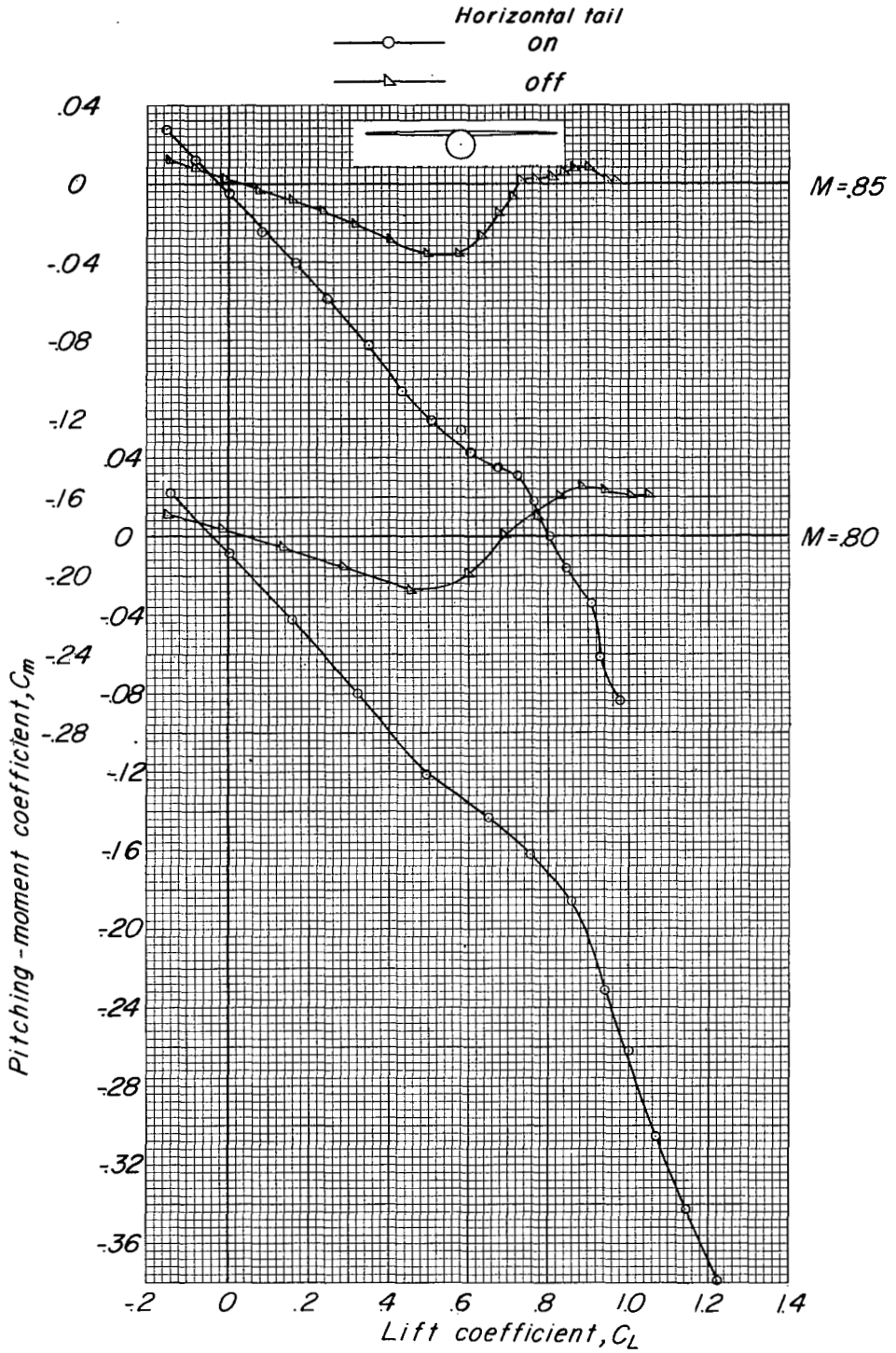

(b) C_m against C_L.

Figure 6.- Continued.

[redacted]

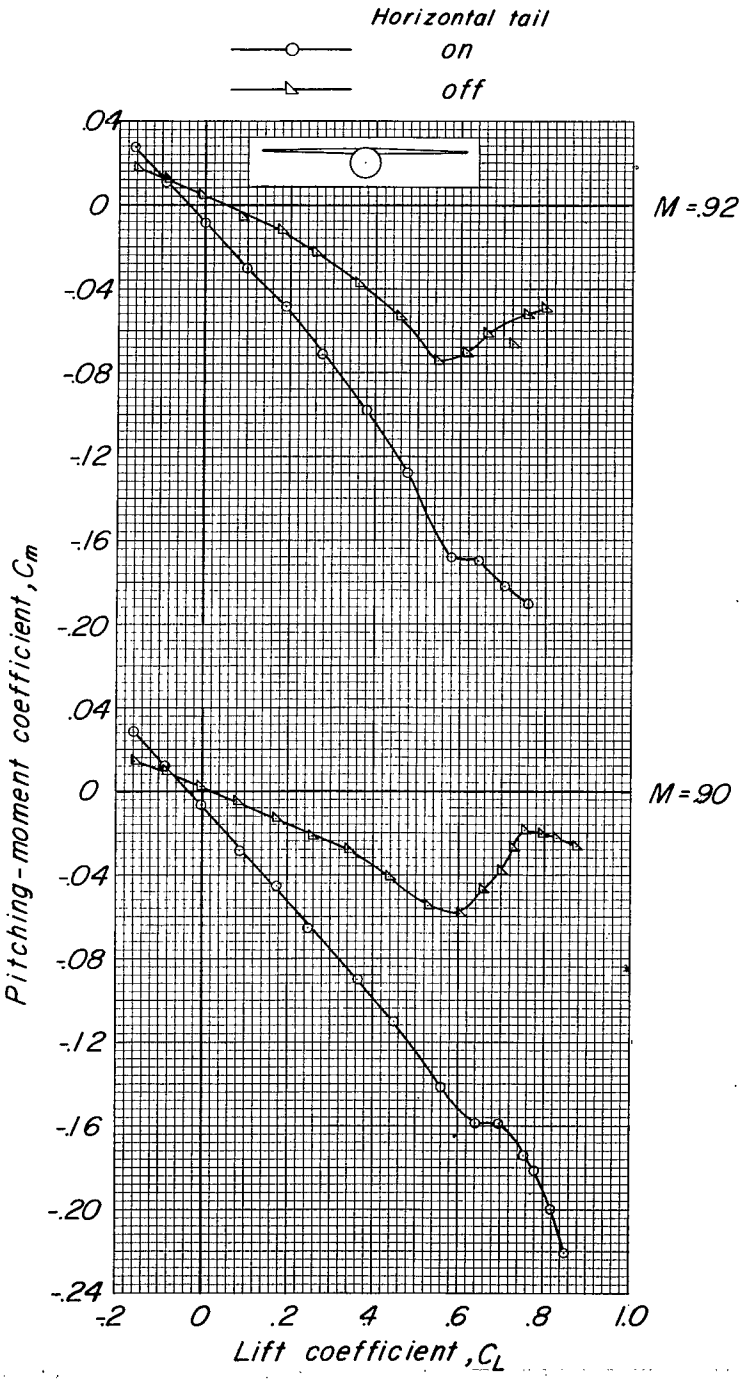

(b) Concluded.

Figure 6.- Continued.

[redacted]

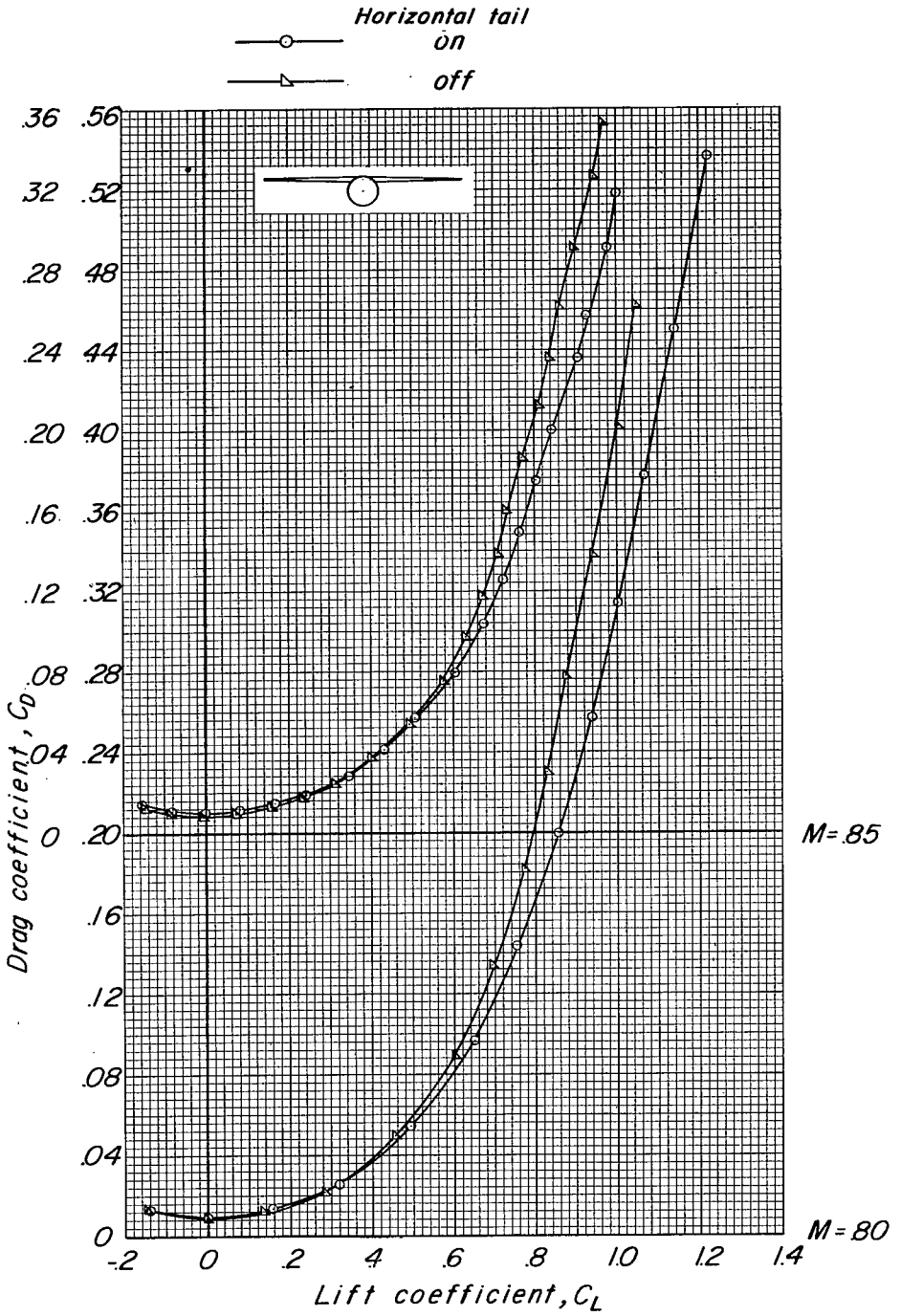

(c) C_D against C_L.

Figure 6.- Continued.

[redacted]

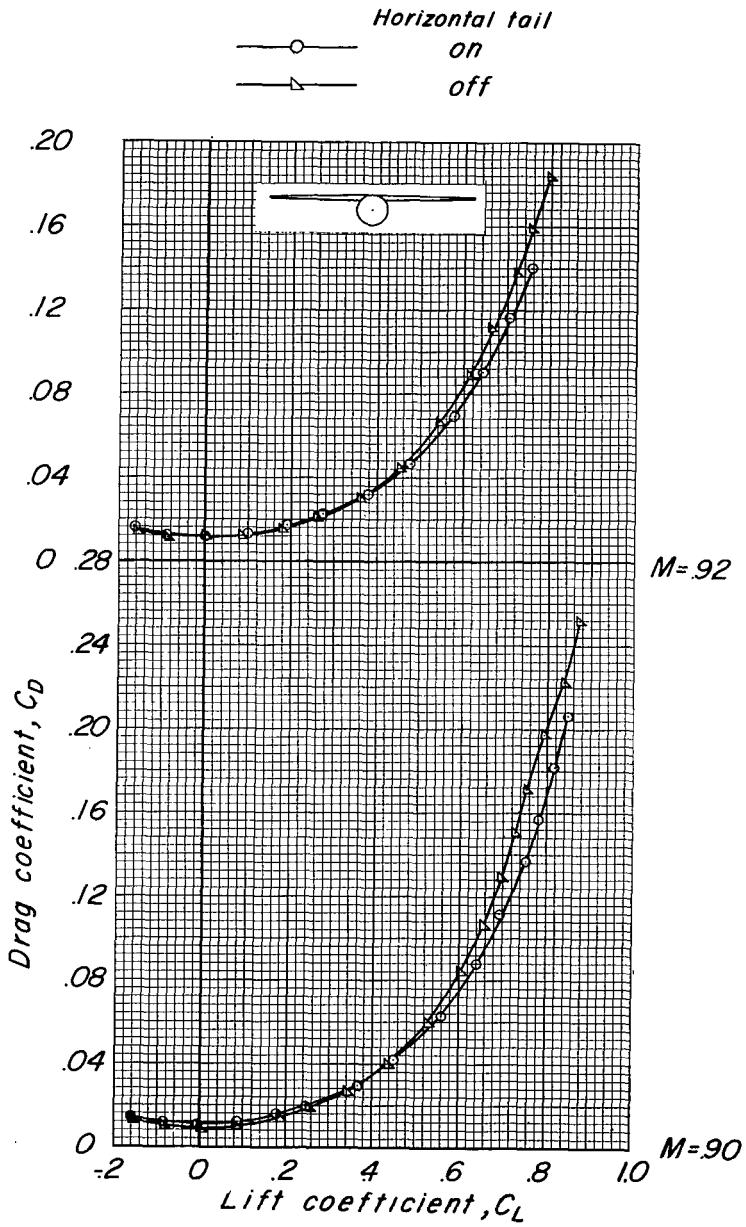

(c) Concluded.

Figure 6.- Concluded.

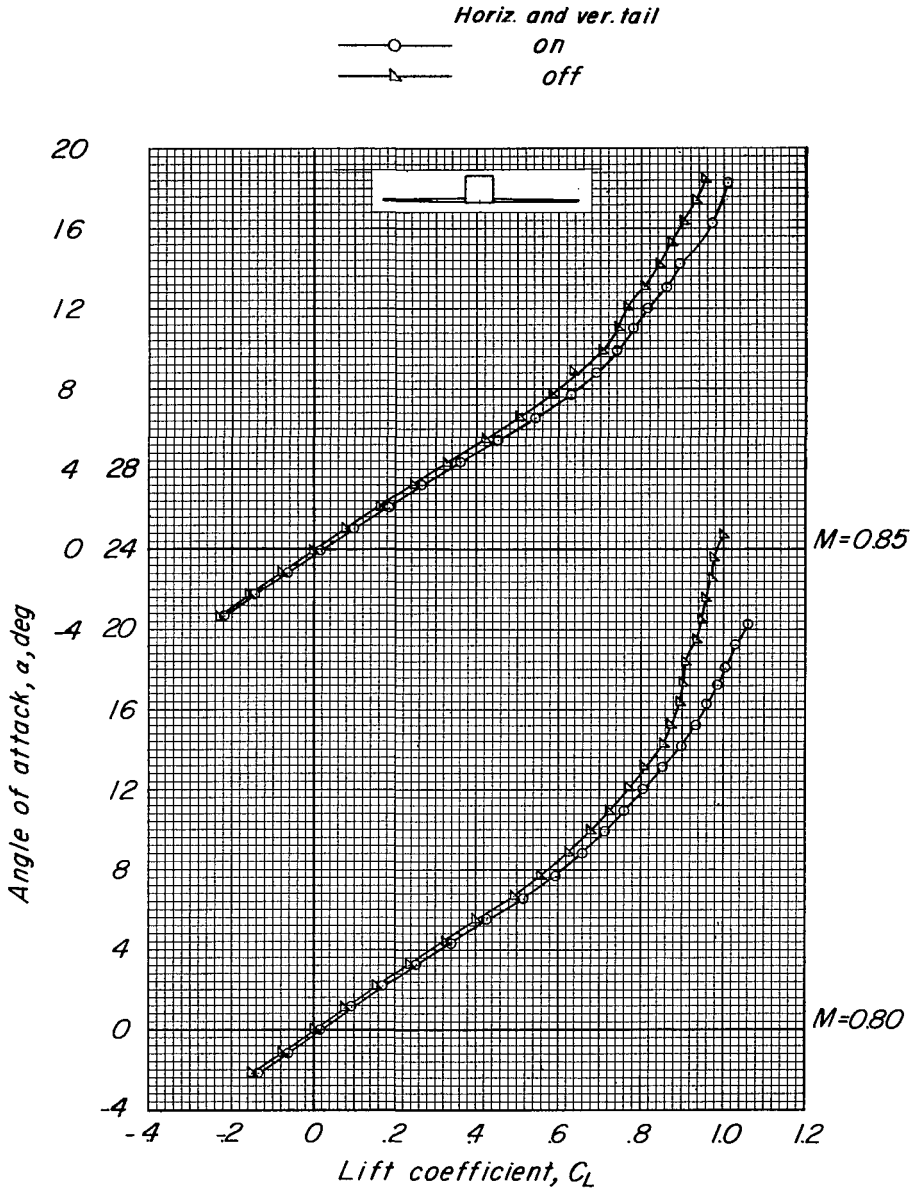

(a) α against C_L.

Figure 7.- Longitudinal characteristics of model with low wing and square fuselage.

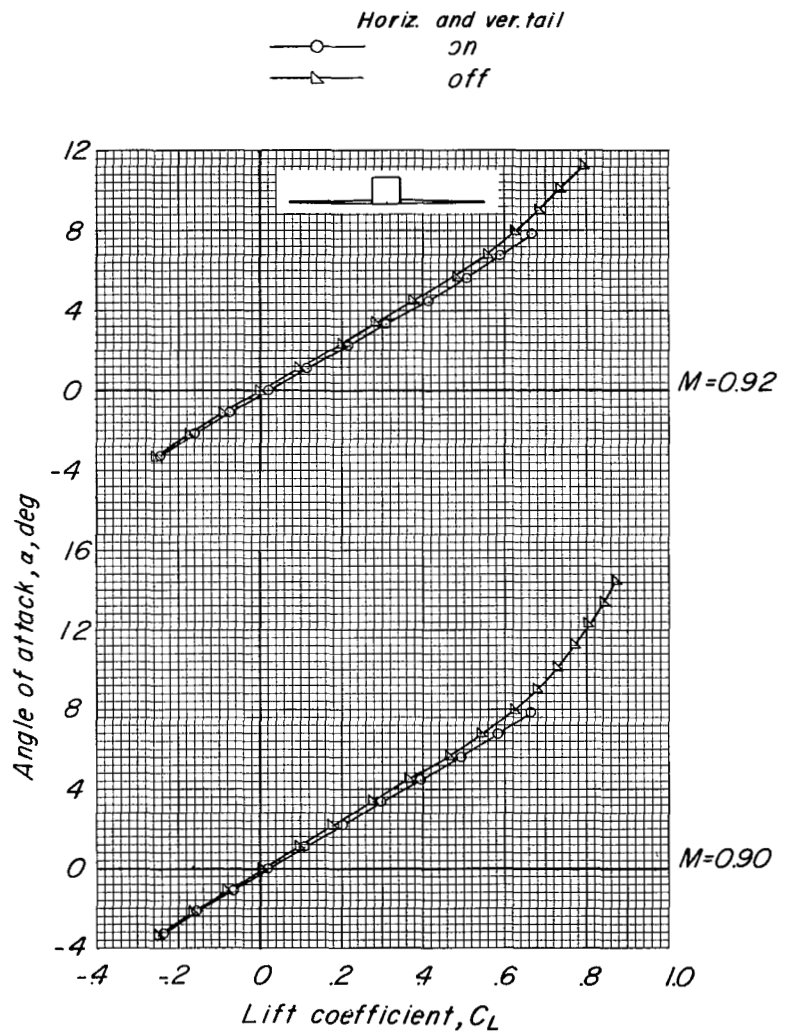

(a) Concluded.

Figure 7.- Continued.

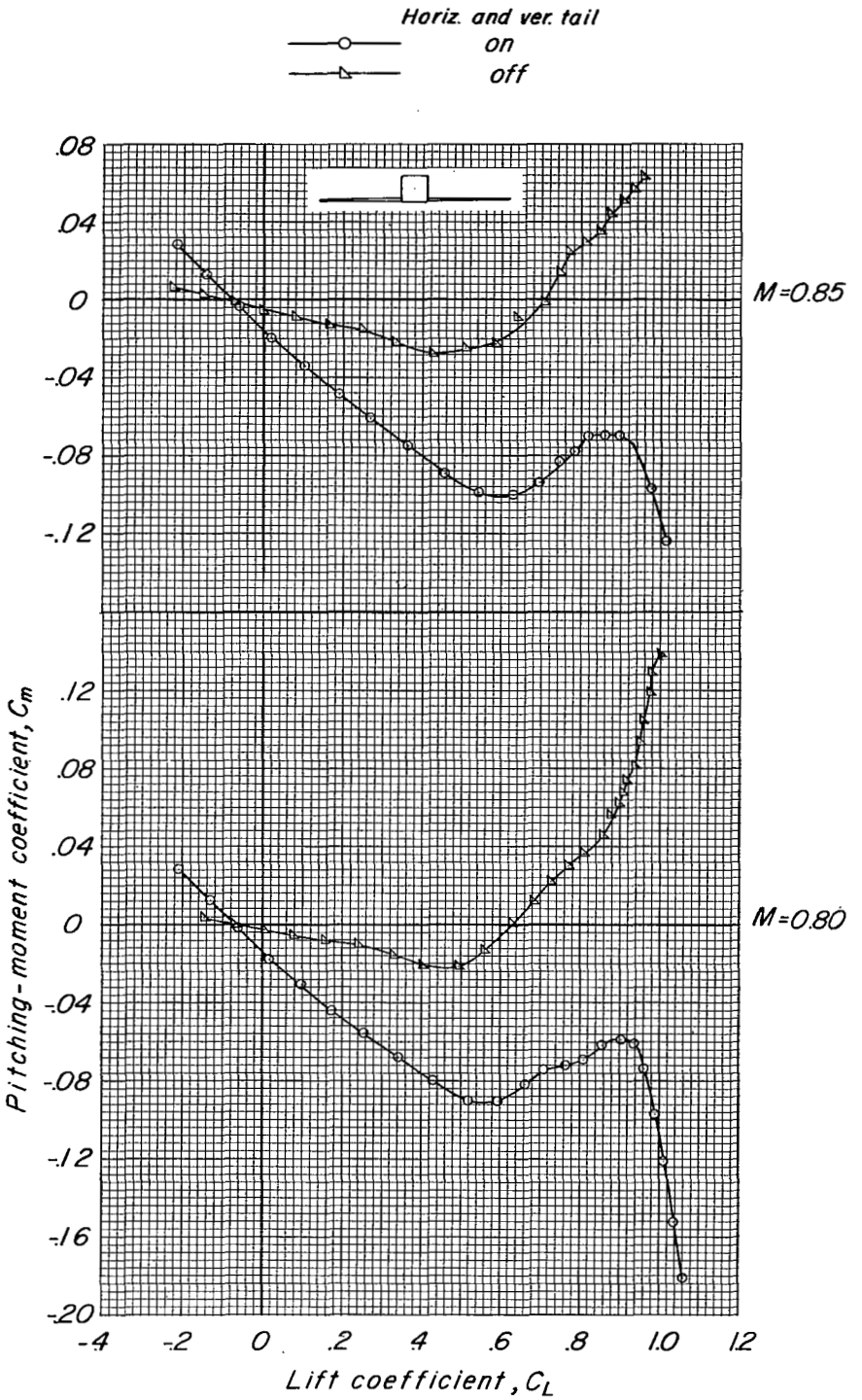

(b) C_m against C_L.

Figure 7.- Continued.

[redacted]

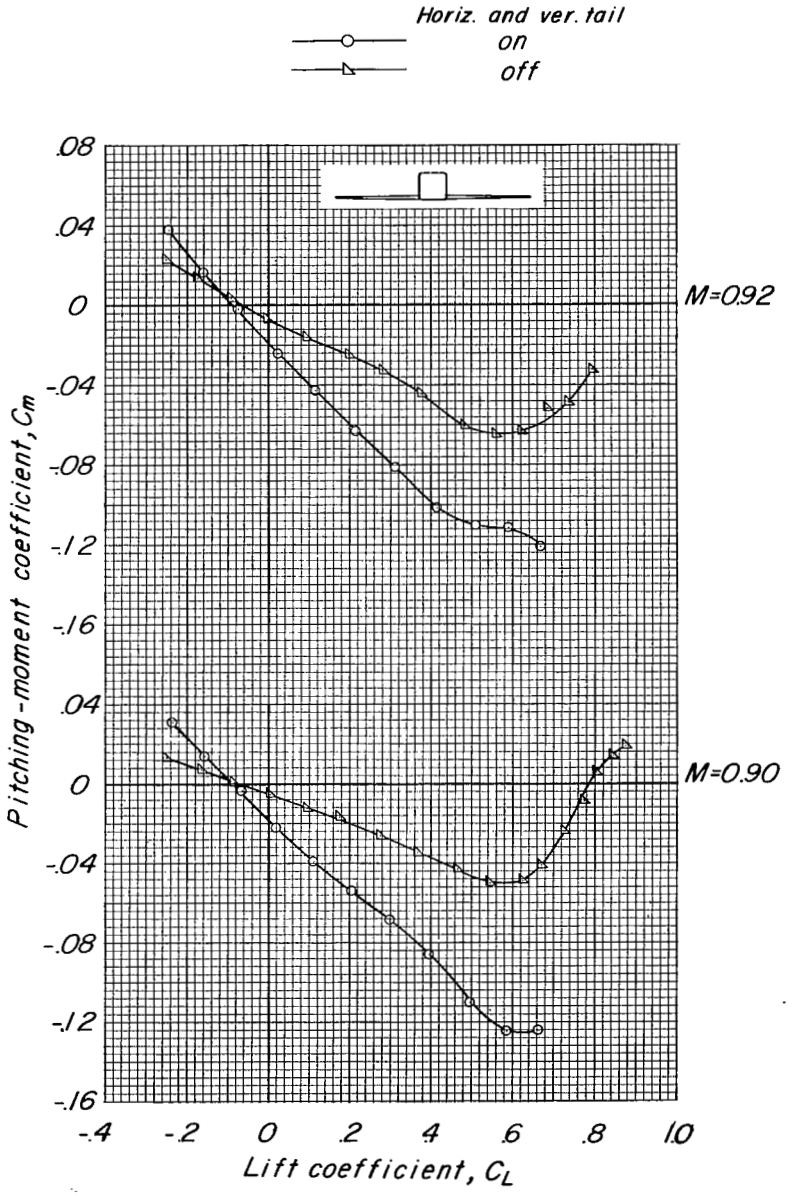

(b) Concluded.

Figure 7.- Continued.

[redacted]

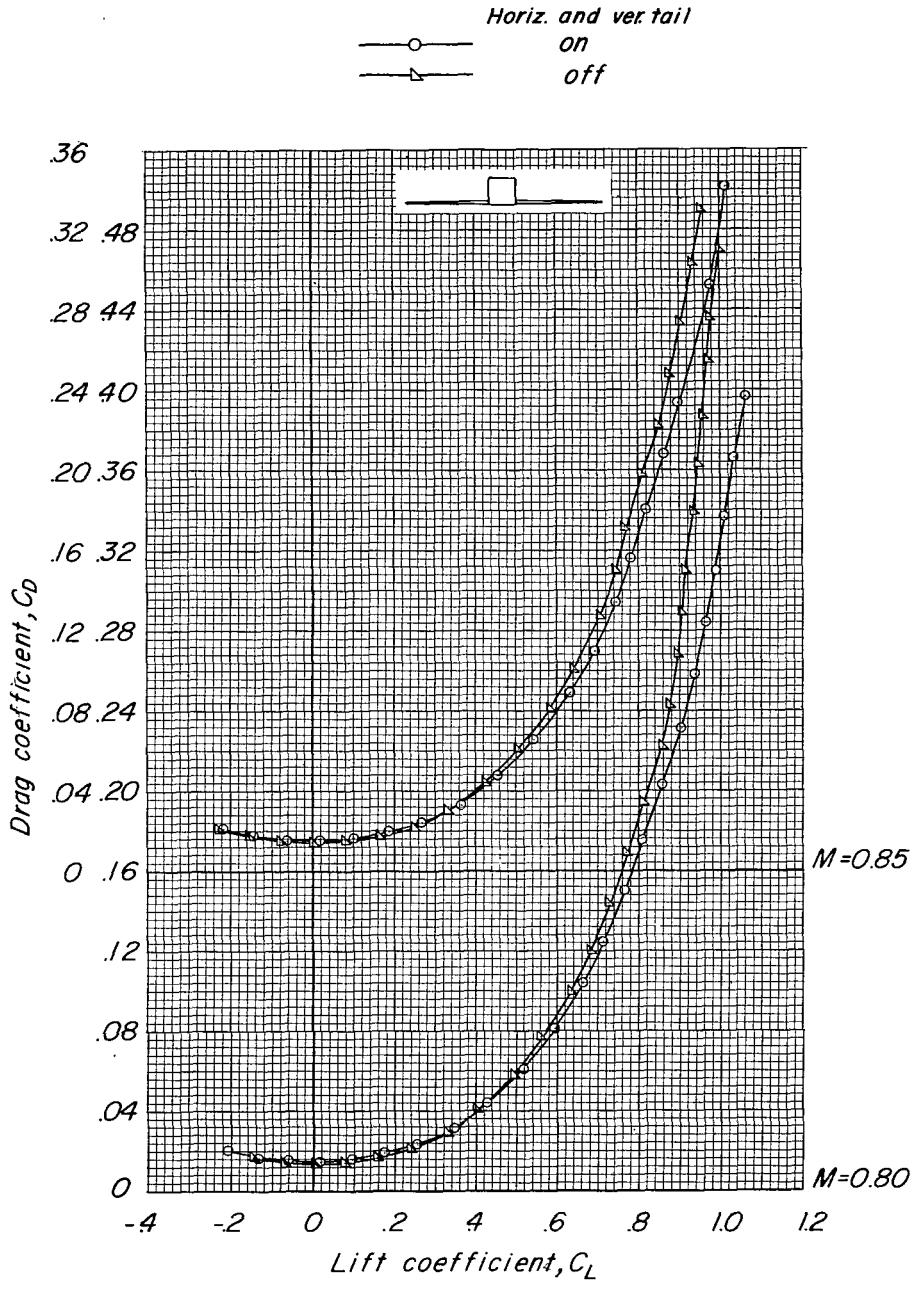

(c) C_D against C_L.

Figure 7.- Continued.

[redacted]

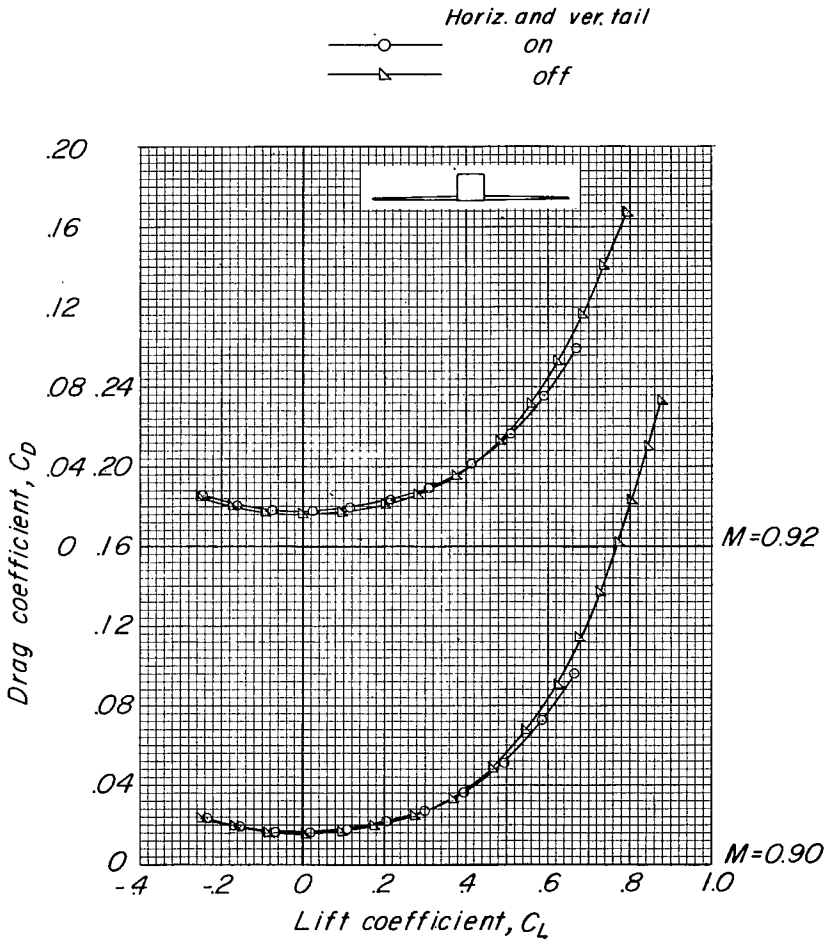

(c) Concluded.

Figure 7.- Concluded.

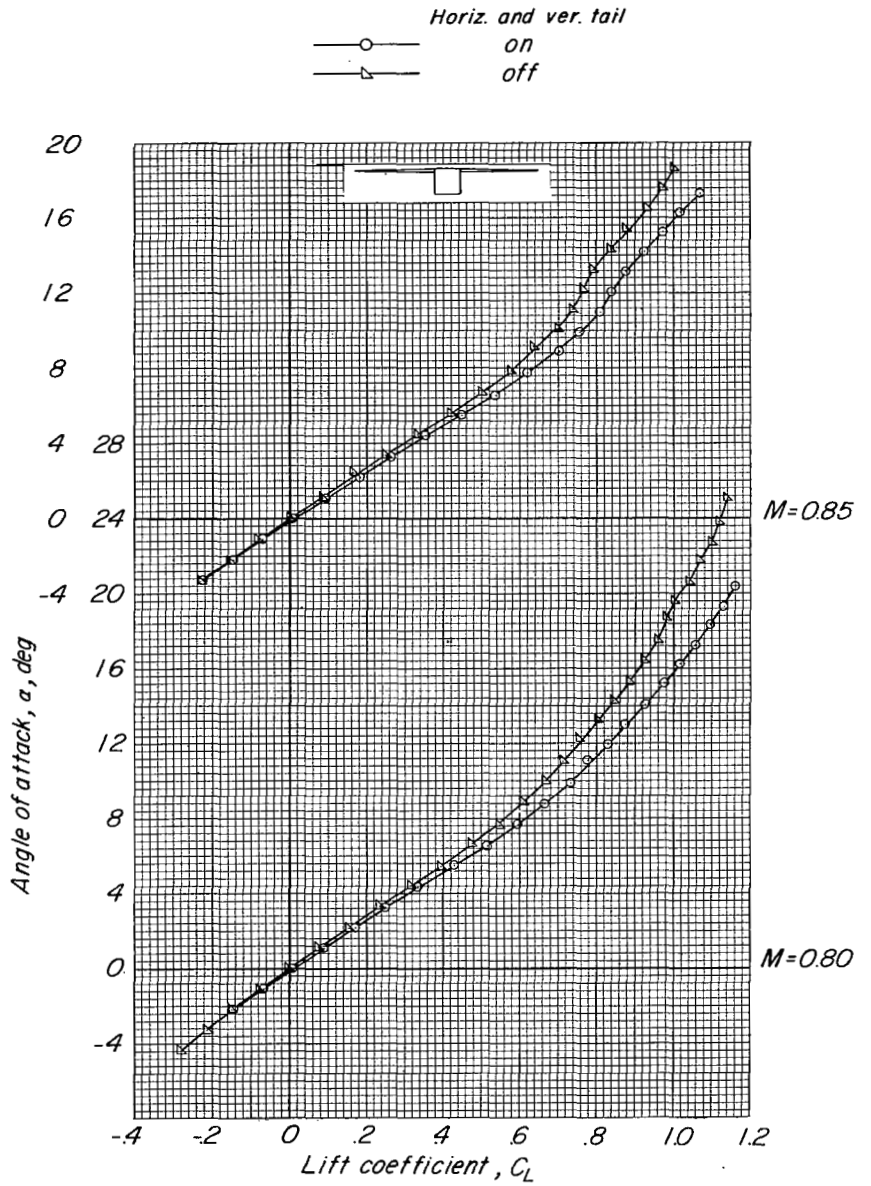

(a) α against C_L.

Figure 8.- Longitudinal characteristics of model with high wing and square fuselage.

[redacted]

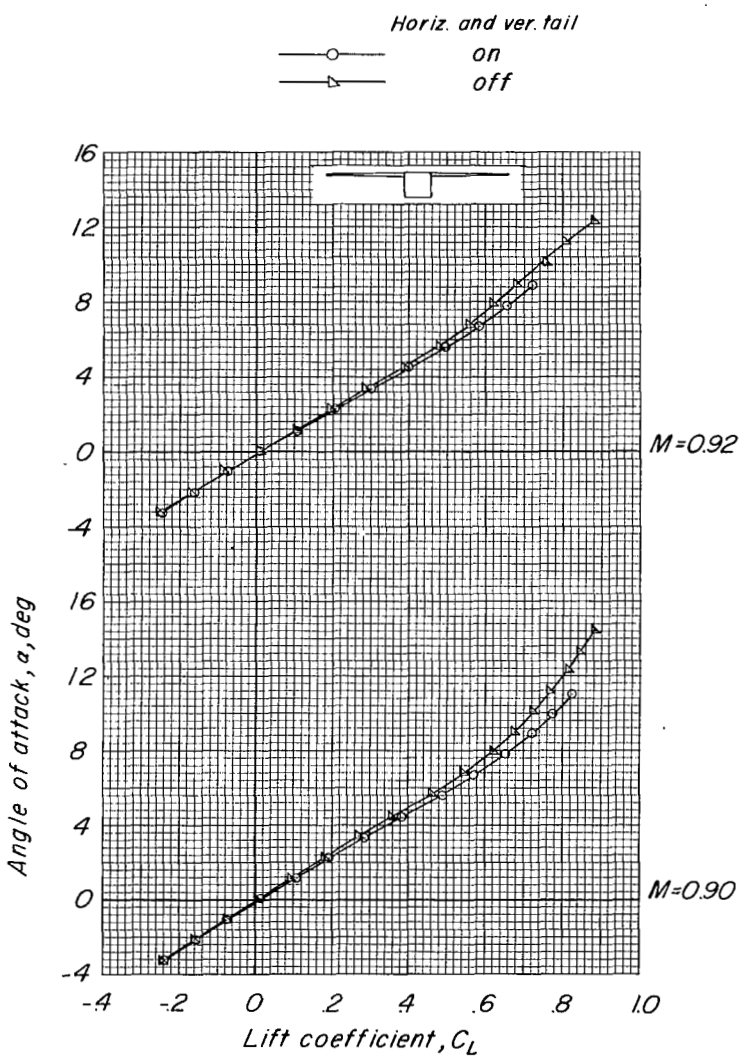

(a) Concluded.

Figure 8.- Continued.

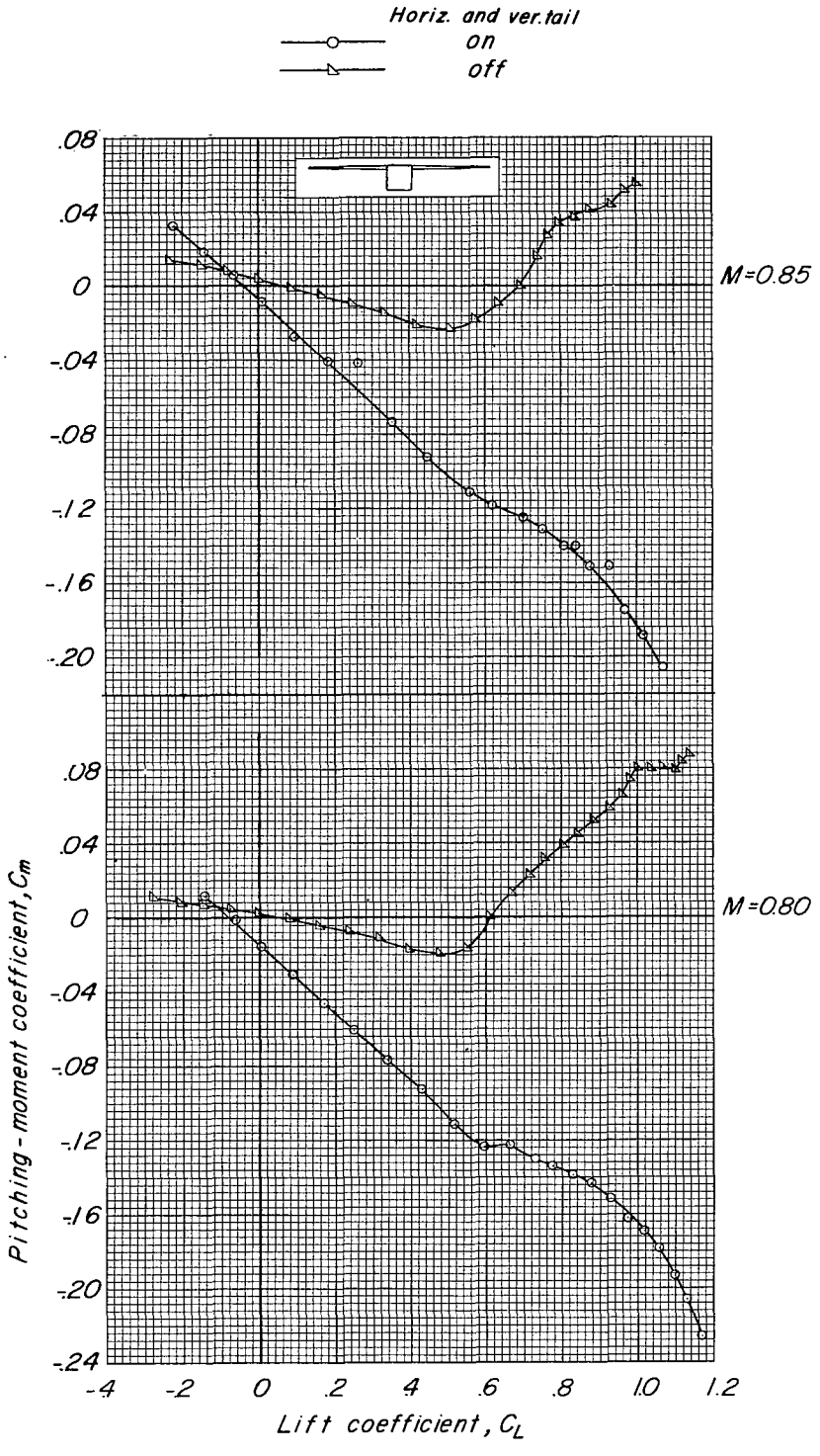

(b) C_m against C_L.

Figure 8.- Continued.

[redacted]

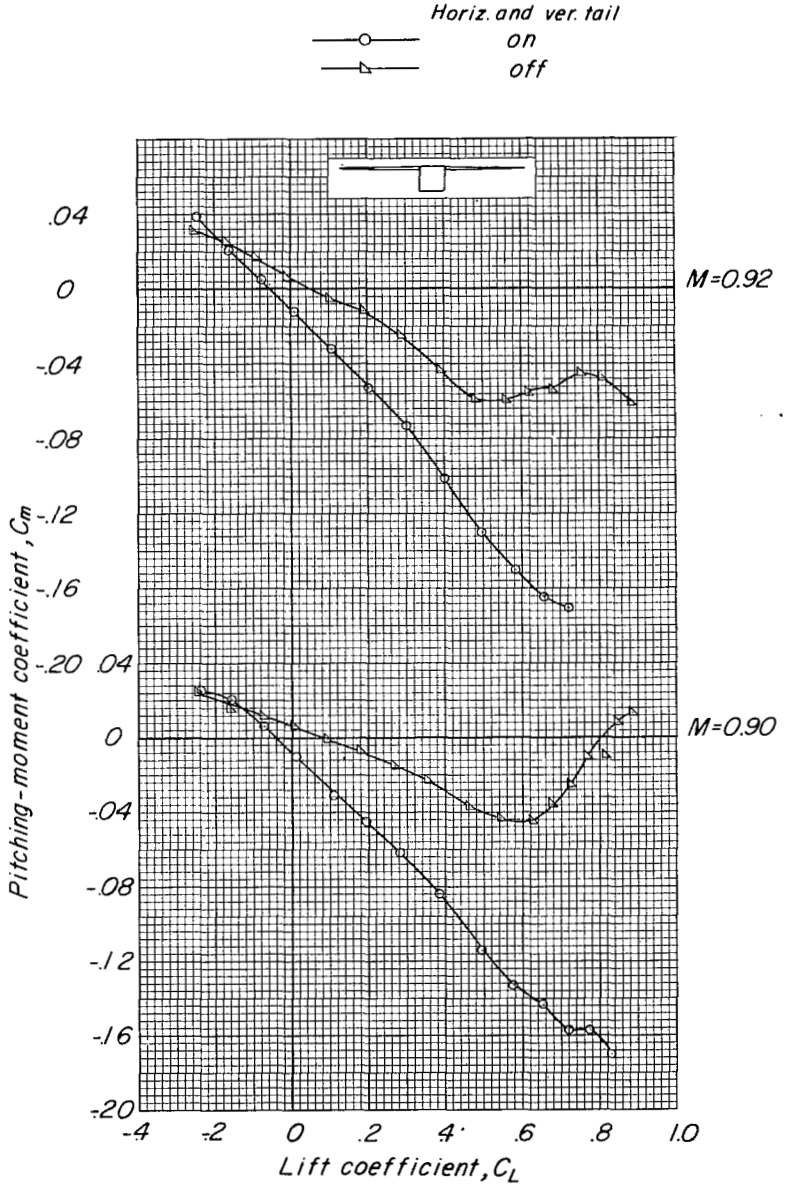

(b) Concluded.

Figure 8.- Continued.

[redacted]

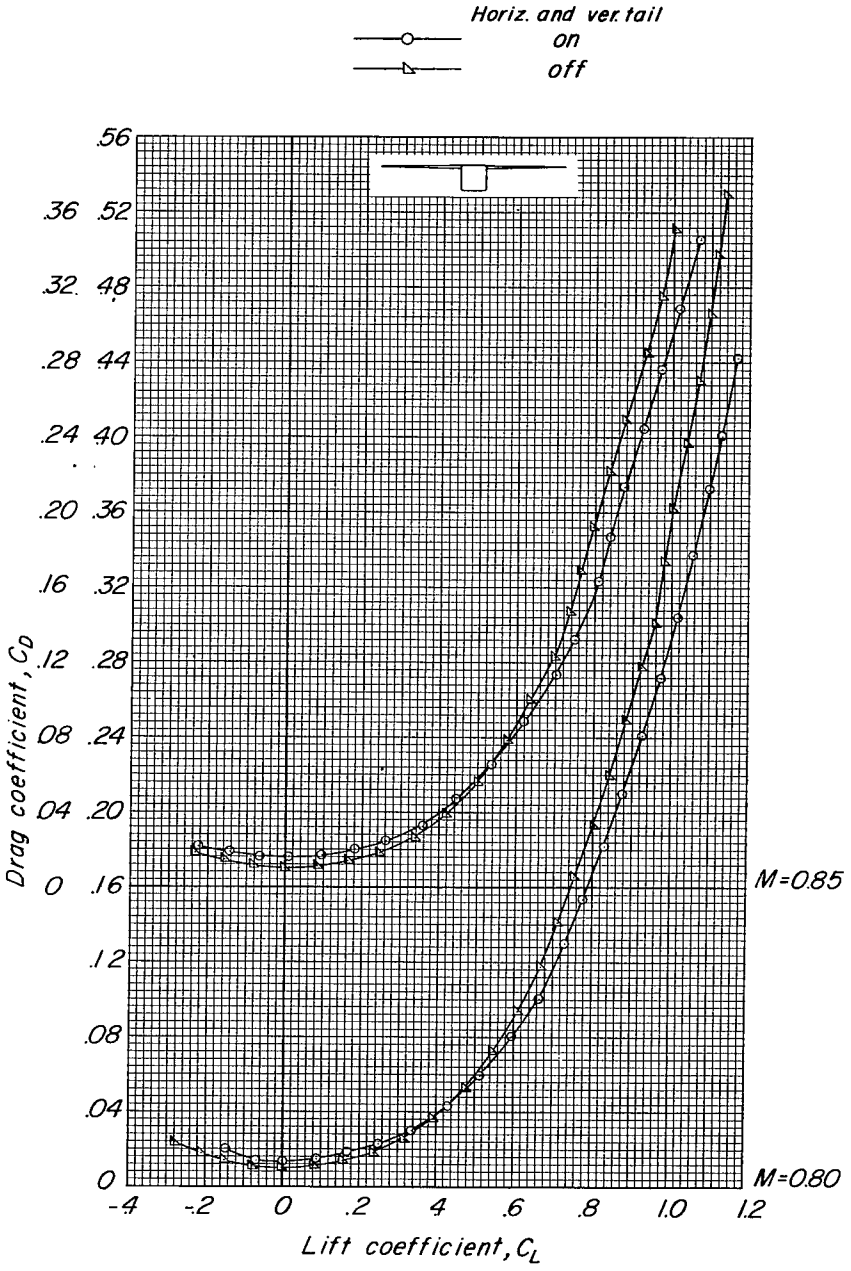

(c) C_D against C_L.

Figure 8.- Continued.

[redacted]

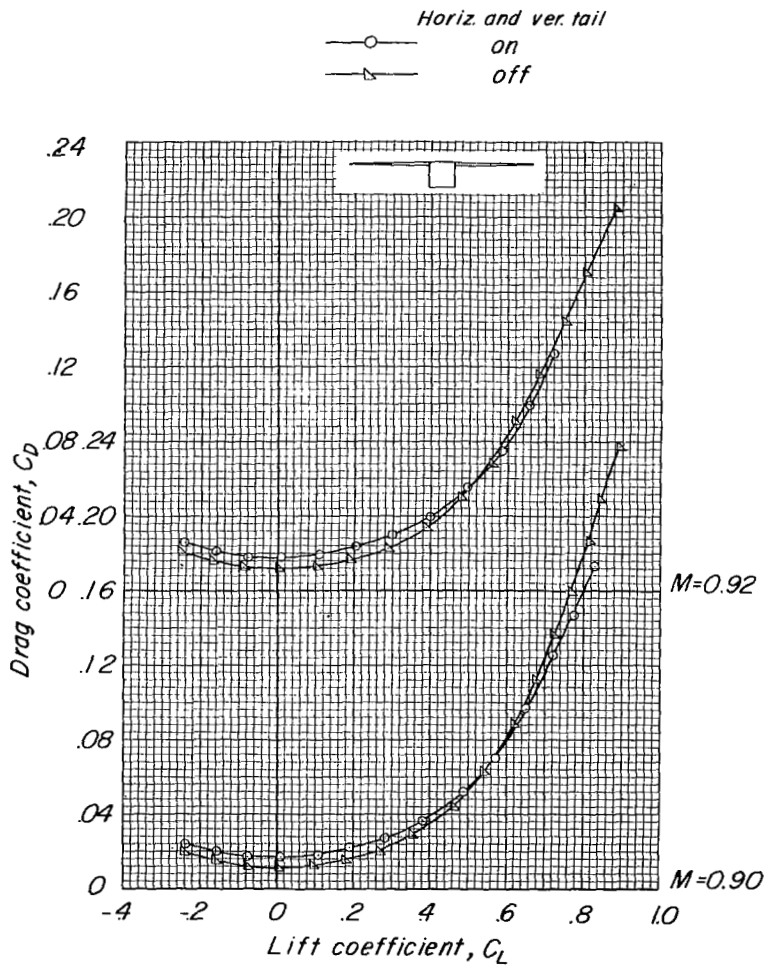

(c) Concluded.

Figure 8.- Concluded.

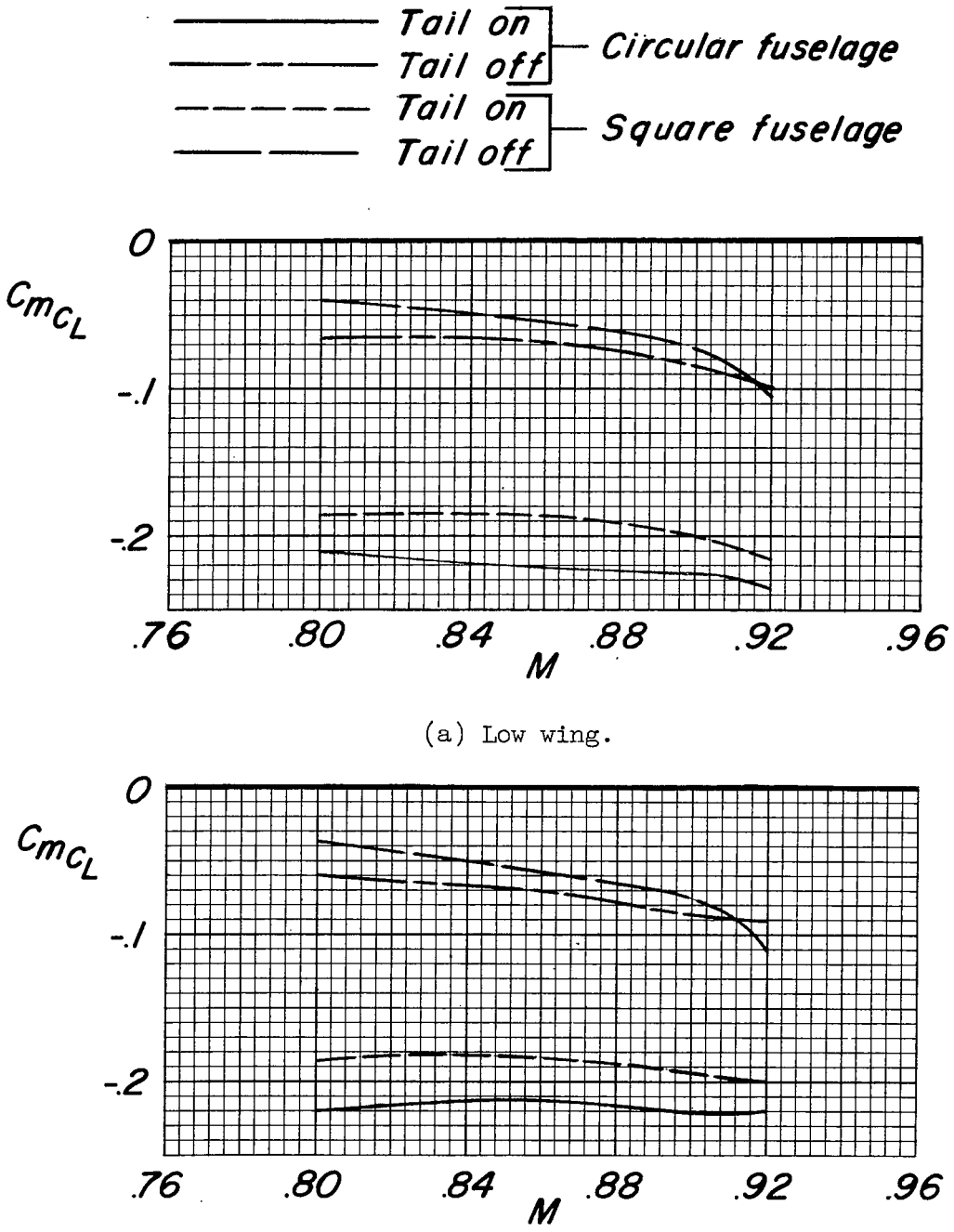

(a) Low wing.

(b) High wing.

Figure 9.- Variation of $C_{m_{C_L}}$ with Mach number. $C_L = 0$.

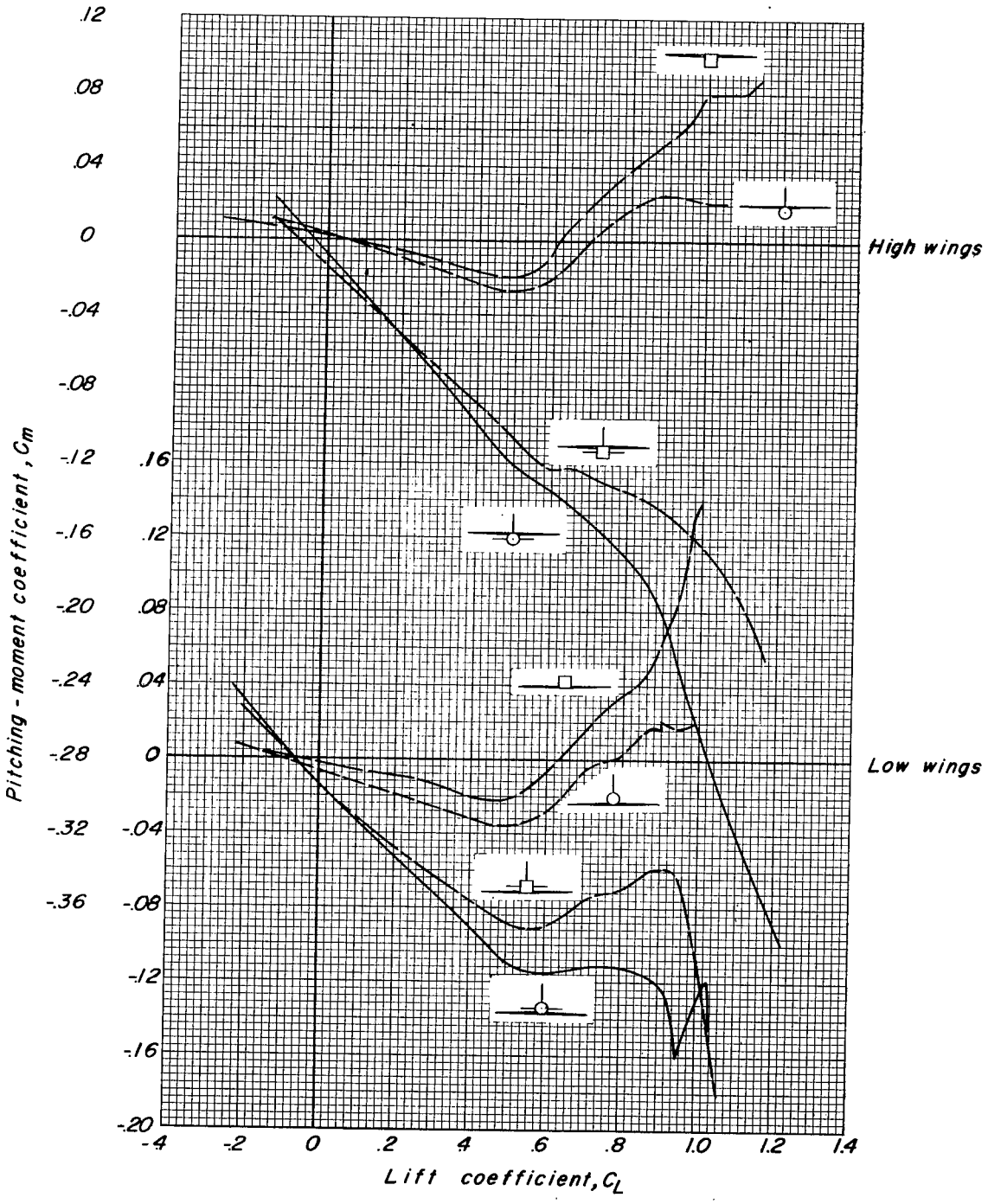

Figure 10.- Comparison of pitching-moment-coefficient variation with lift coefficient of circular and square cross-section fuselage models. M = 0.80.

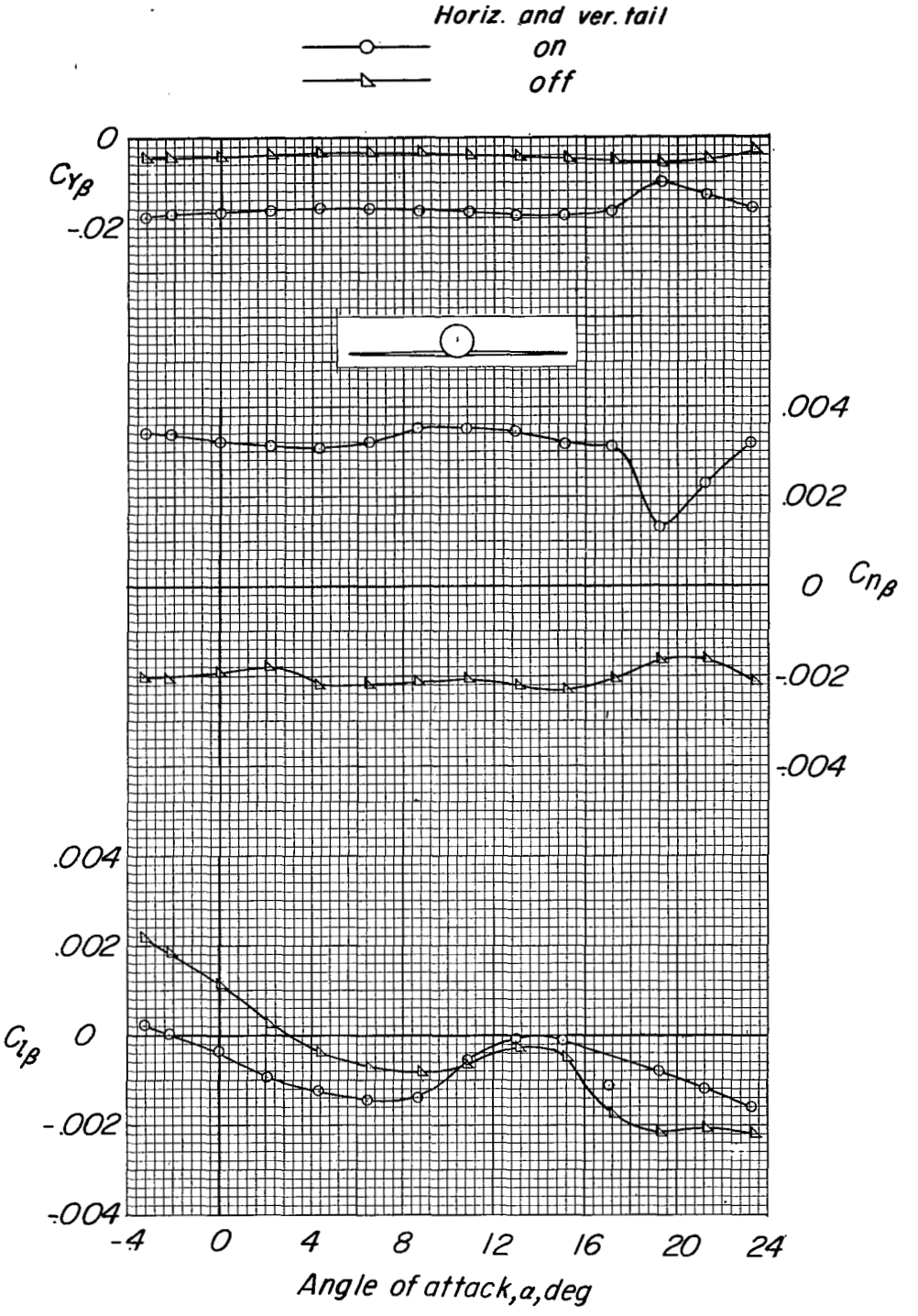

(a) M = 0.80.

Figure 11.- Lateral stability parameter characteristics of model with low wing and circular fuselage.

[redacted]

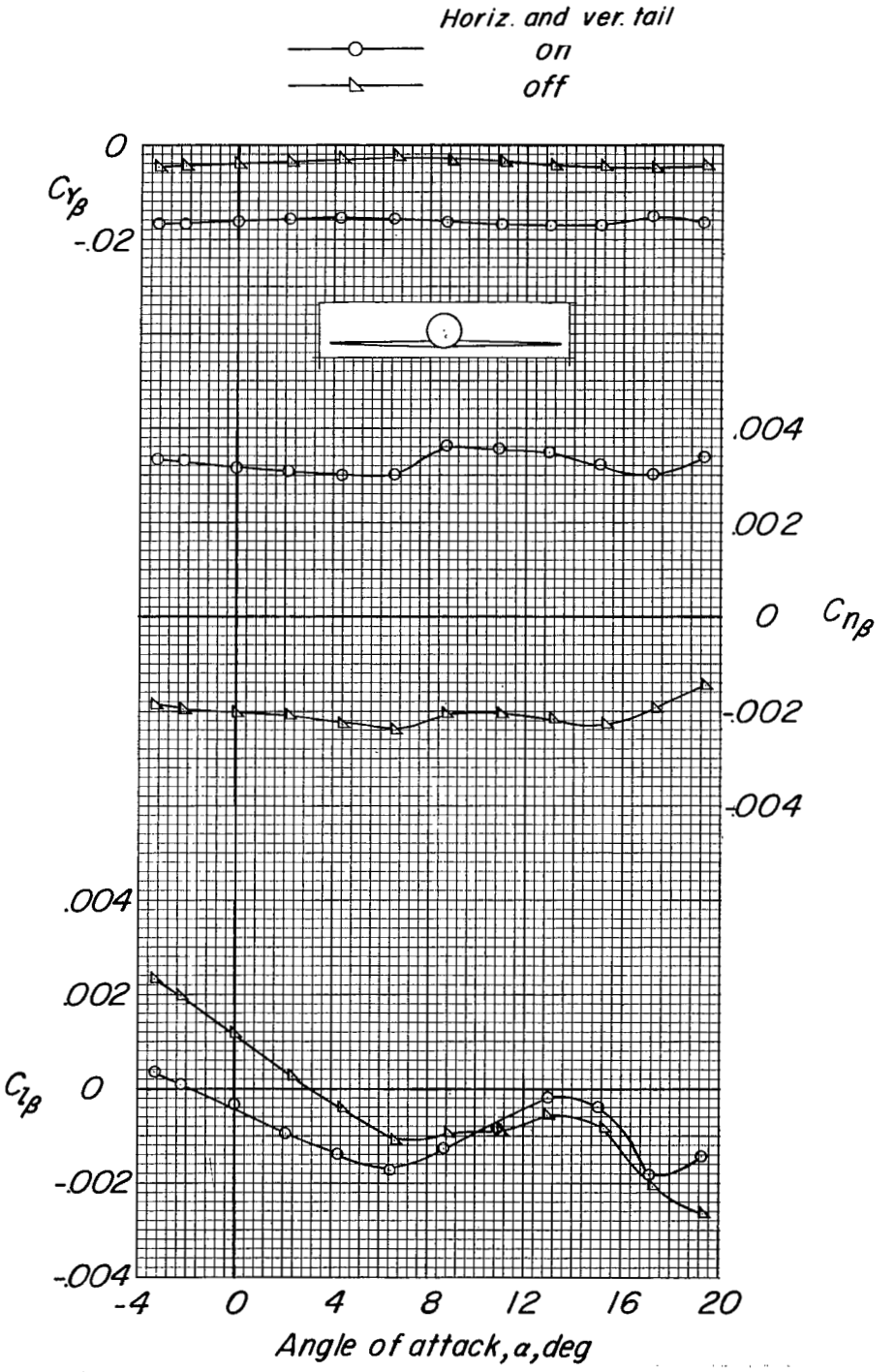

(b) M = 0.85.

Figure 11.- Continued.

[redacted]

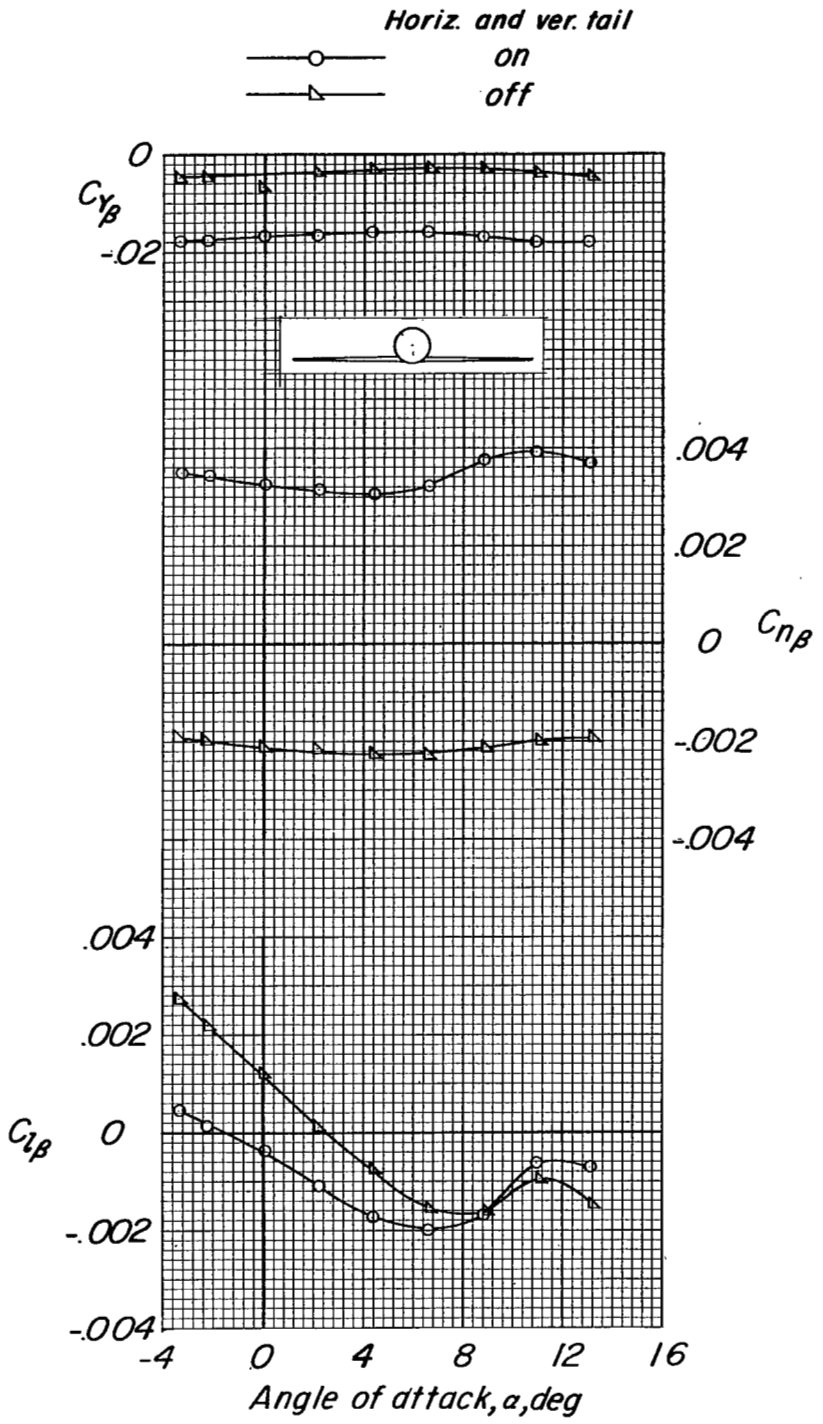

(c) M = 0.90.

Figure 11.- Continued.

[redacted]

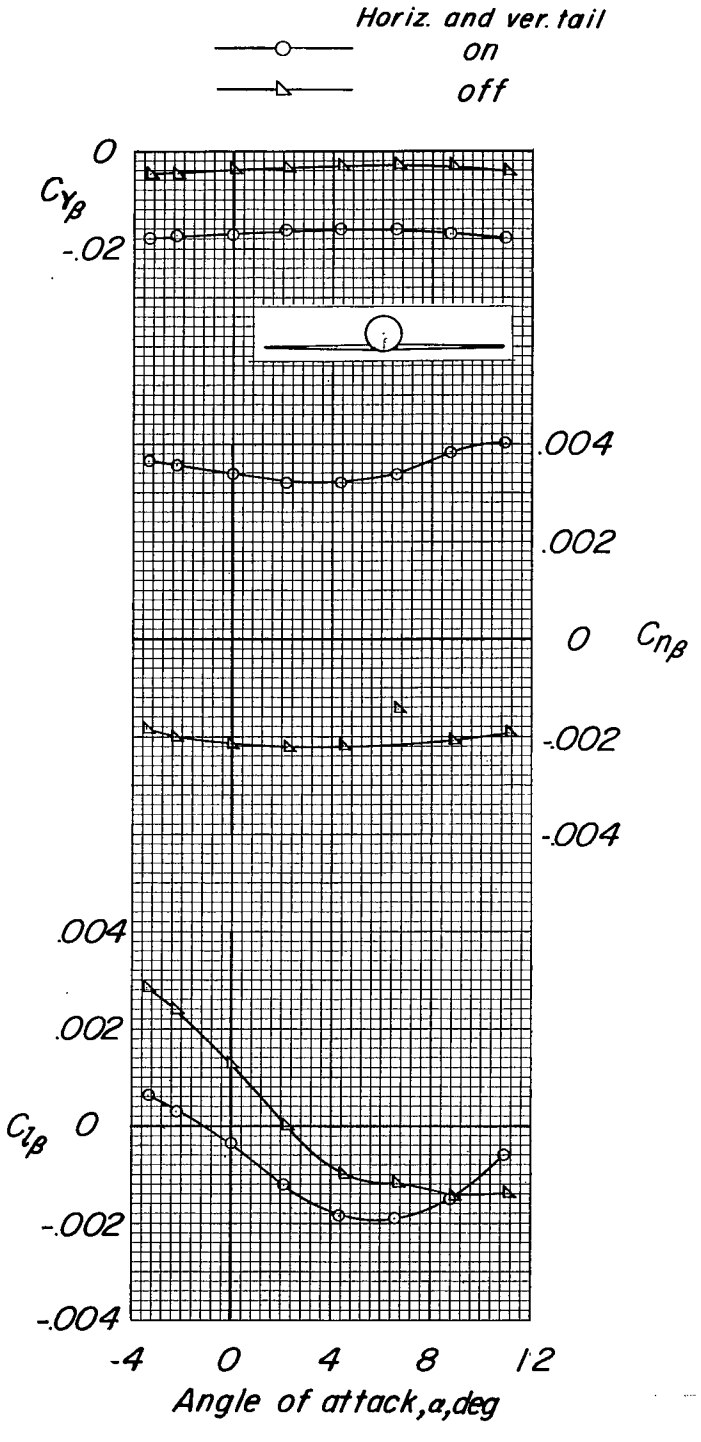

(d) M = 0.92.

Figure 11.- Concluded.

[redacted]

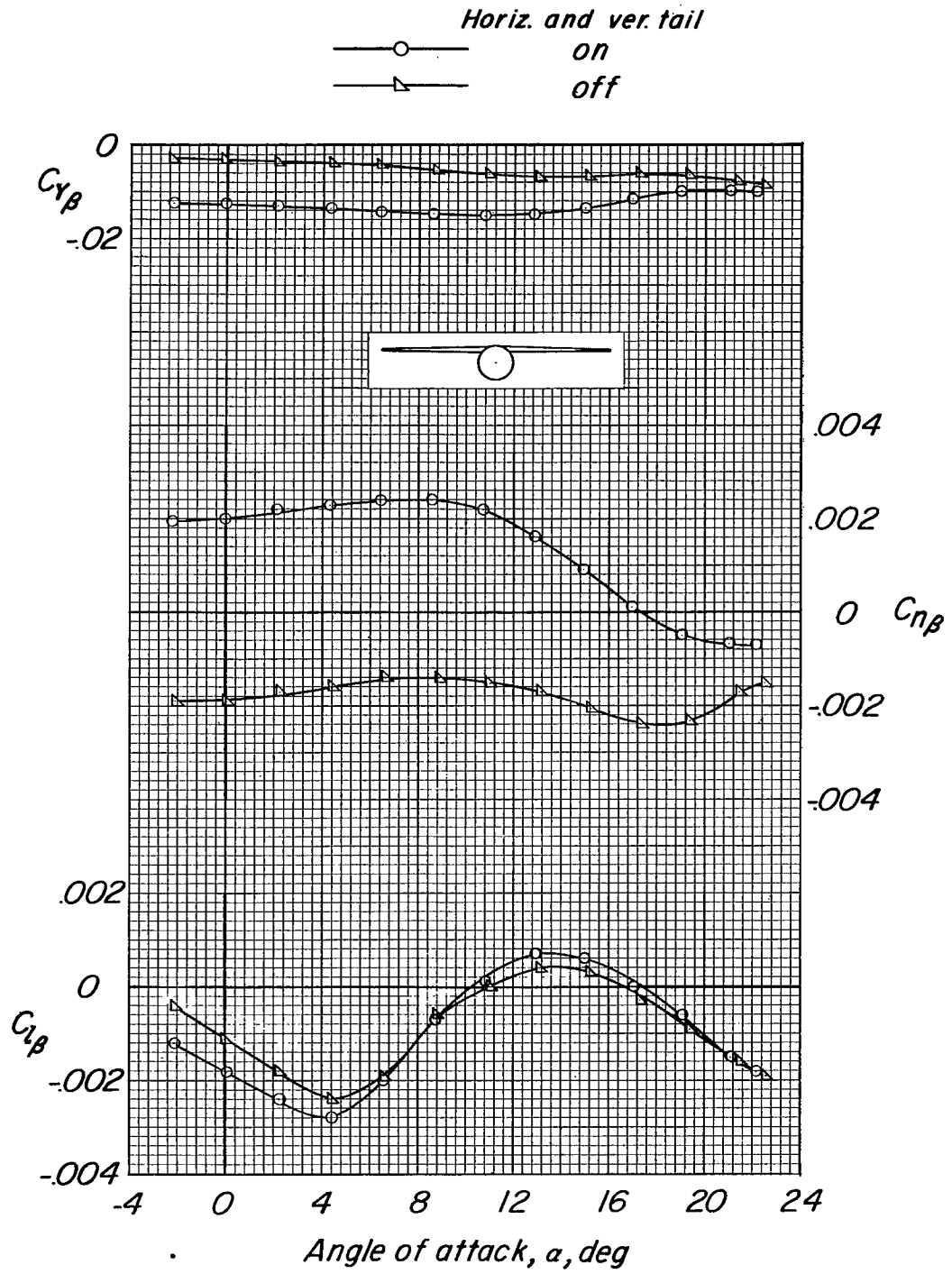

(a) M = 0.80.

Figure 12.- Lateral stability parameter characteristics of model with high wing and circular fuselage.

[redacted]

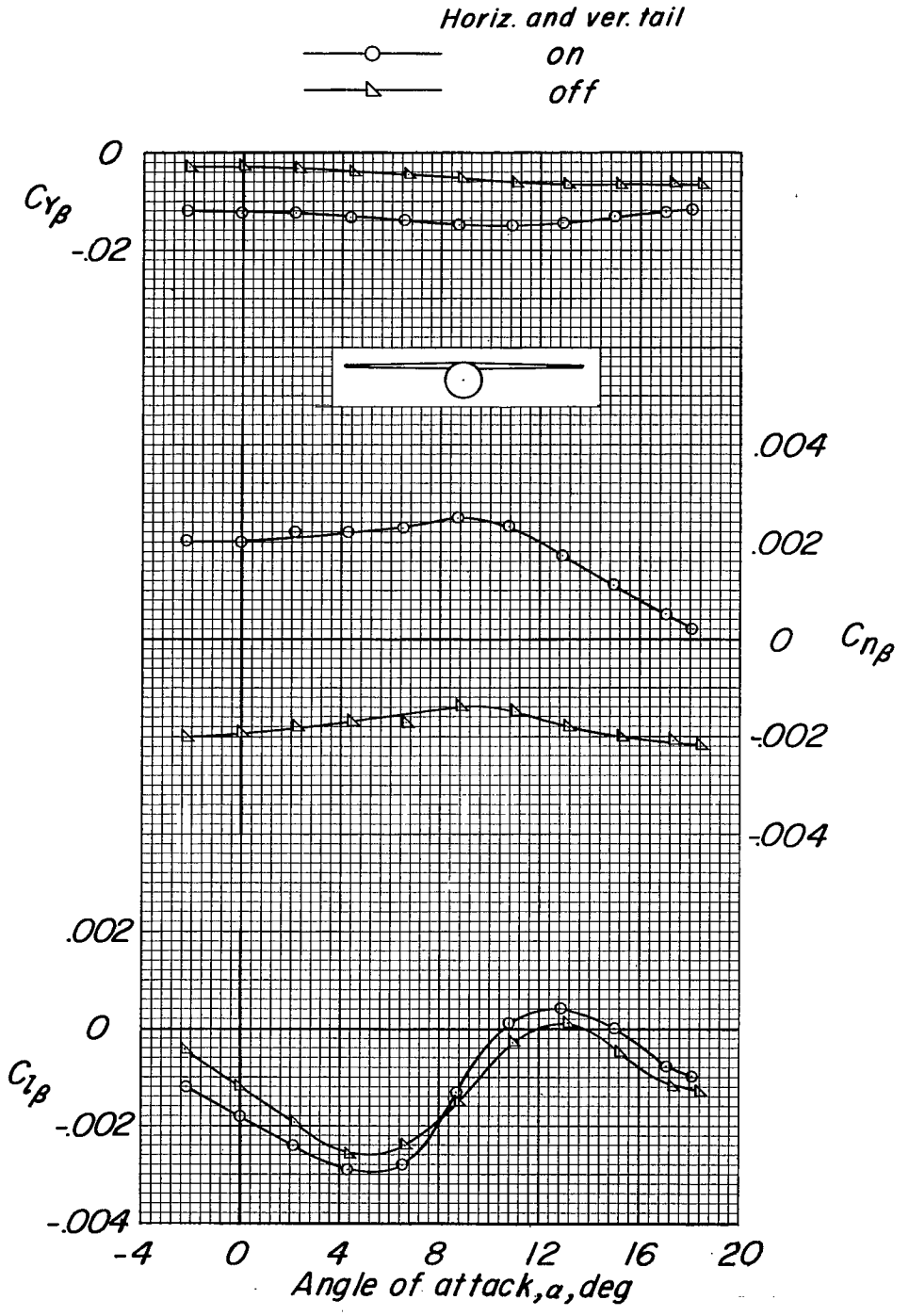

(b) M = 0.85.

Figure 12.- Continued.

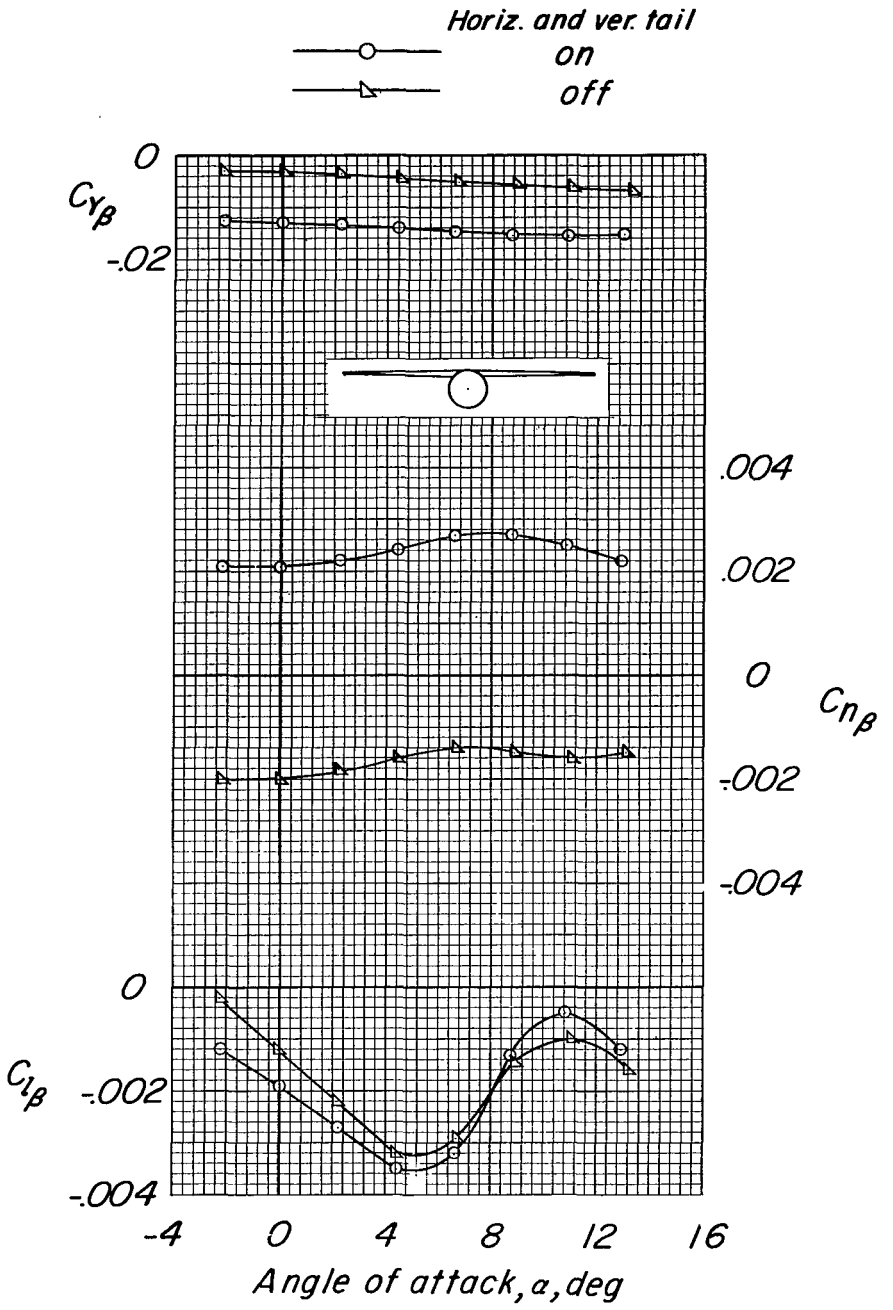

(c) M = 0.90.

Figure 12.- Continued.

[redacted]

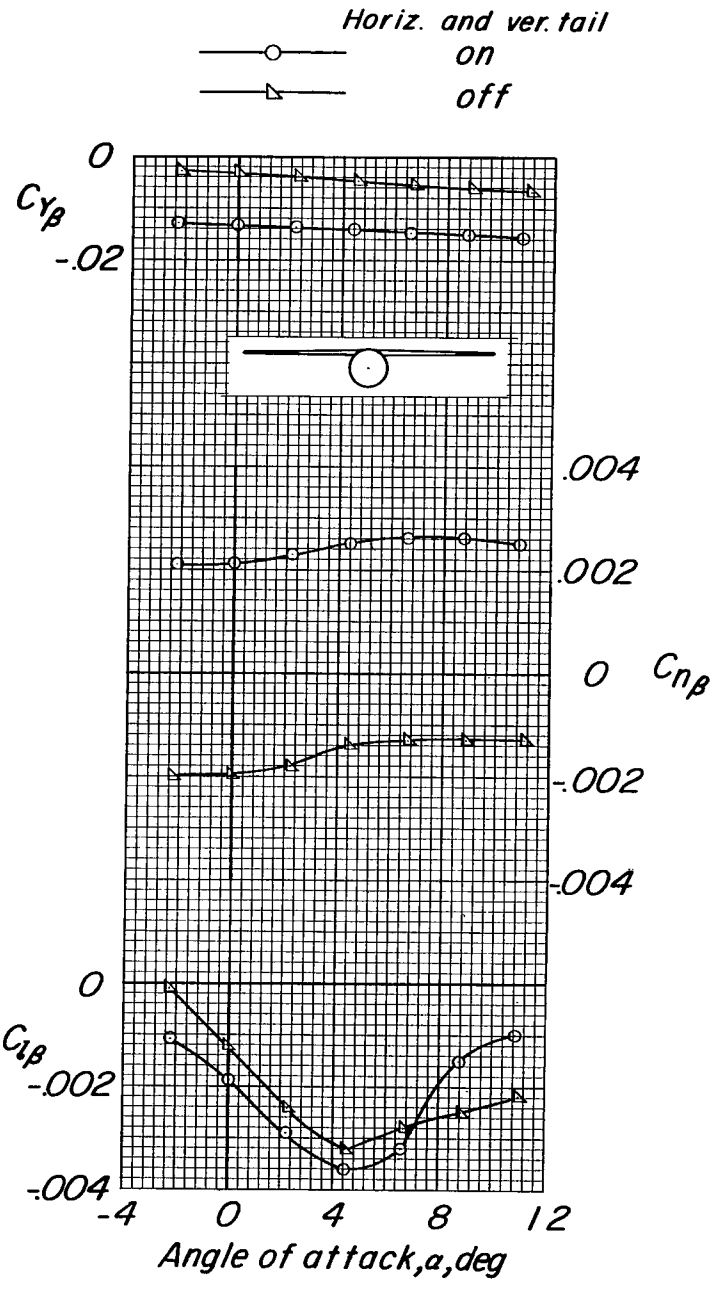

(d) M = 0.92.

Figure 12.- Concluded.

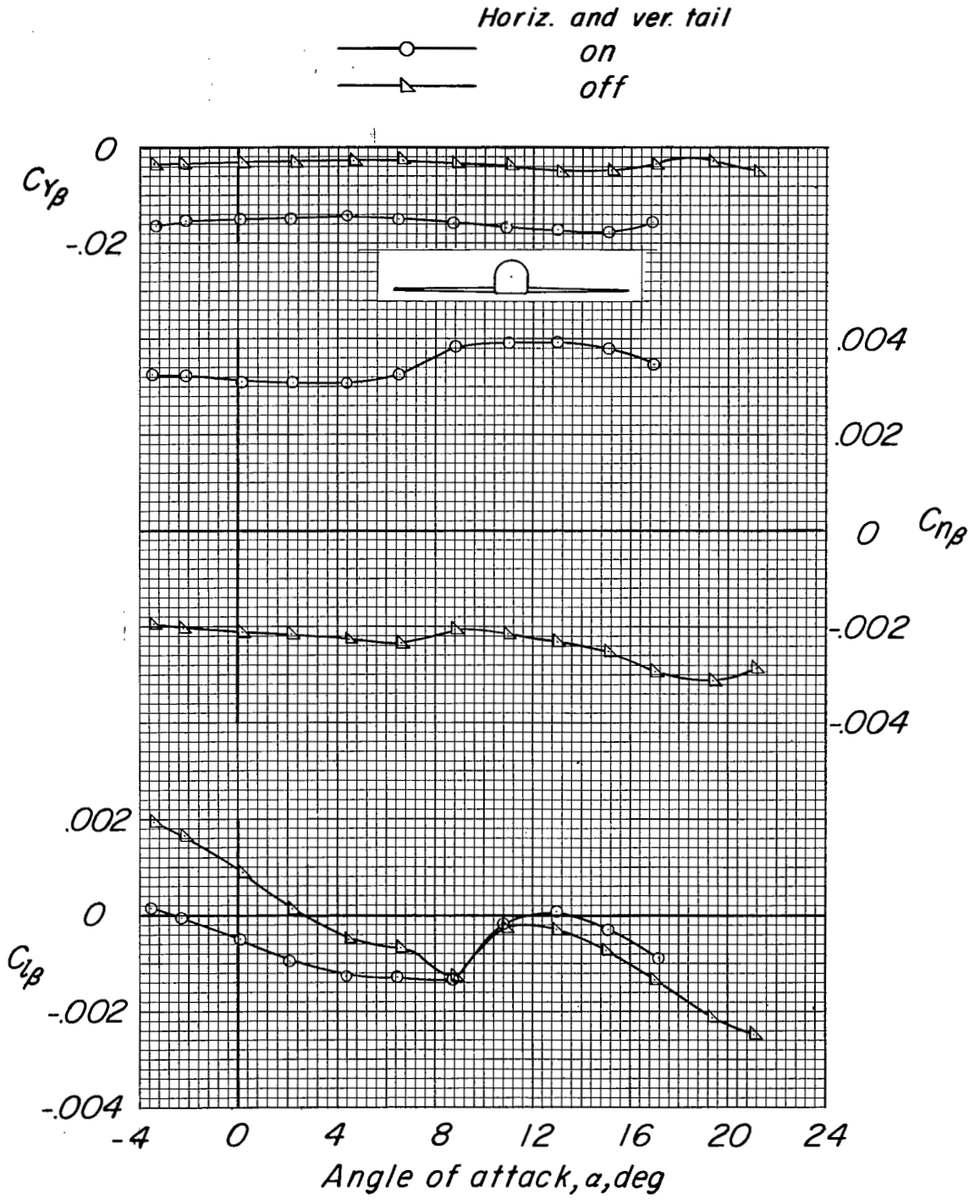

(a) M = 0.80.

Figure 13.- Lateral stability parameter characteristics of model with low wing and half-circular-half-square fuselage.

[redacted]

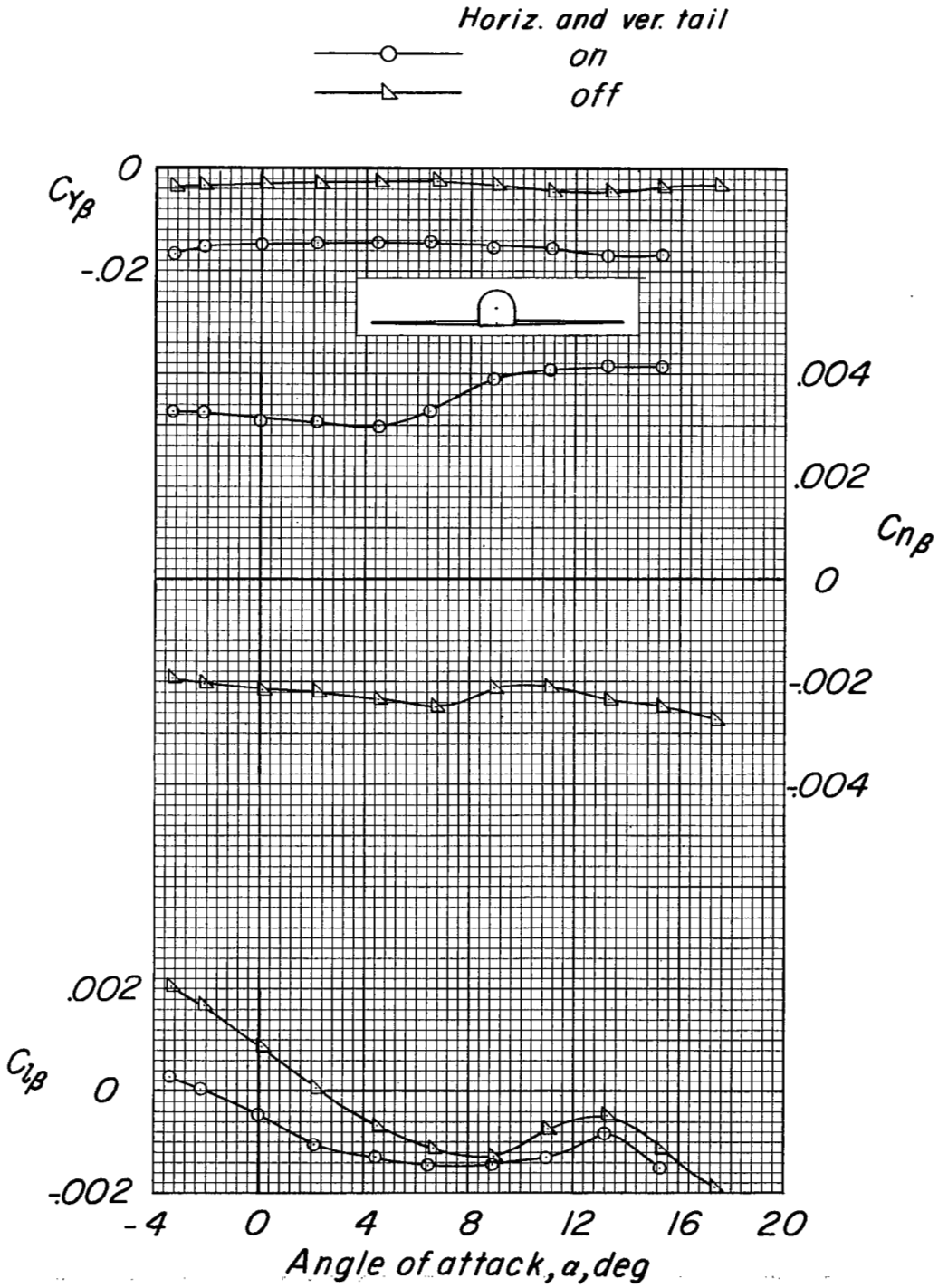

(b) M = 0.85.

Figure 13.- Continued.

[redacted]

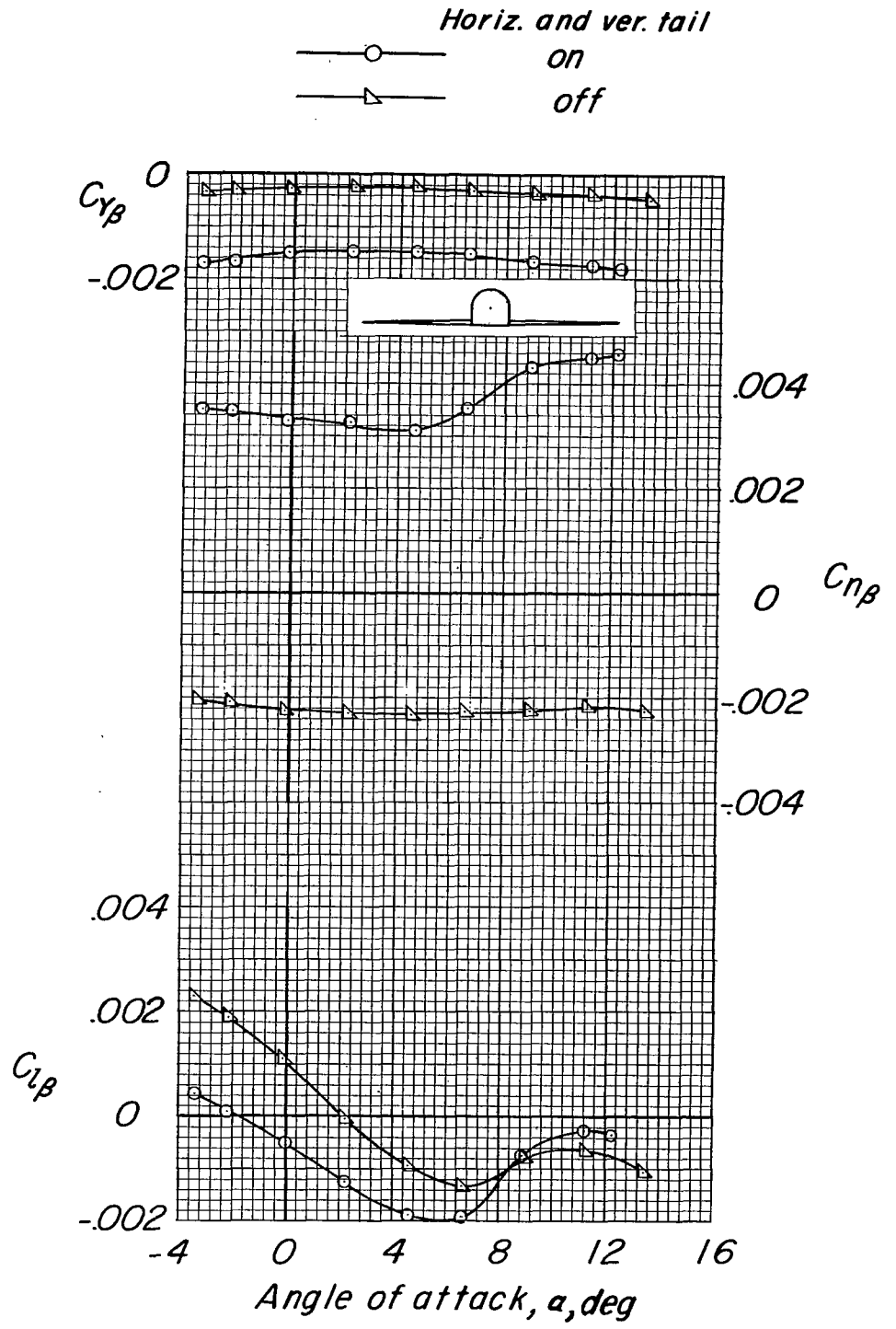

(c) M = 0.90.

Figure 13.- Continued.

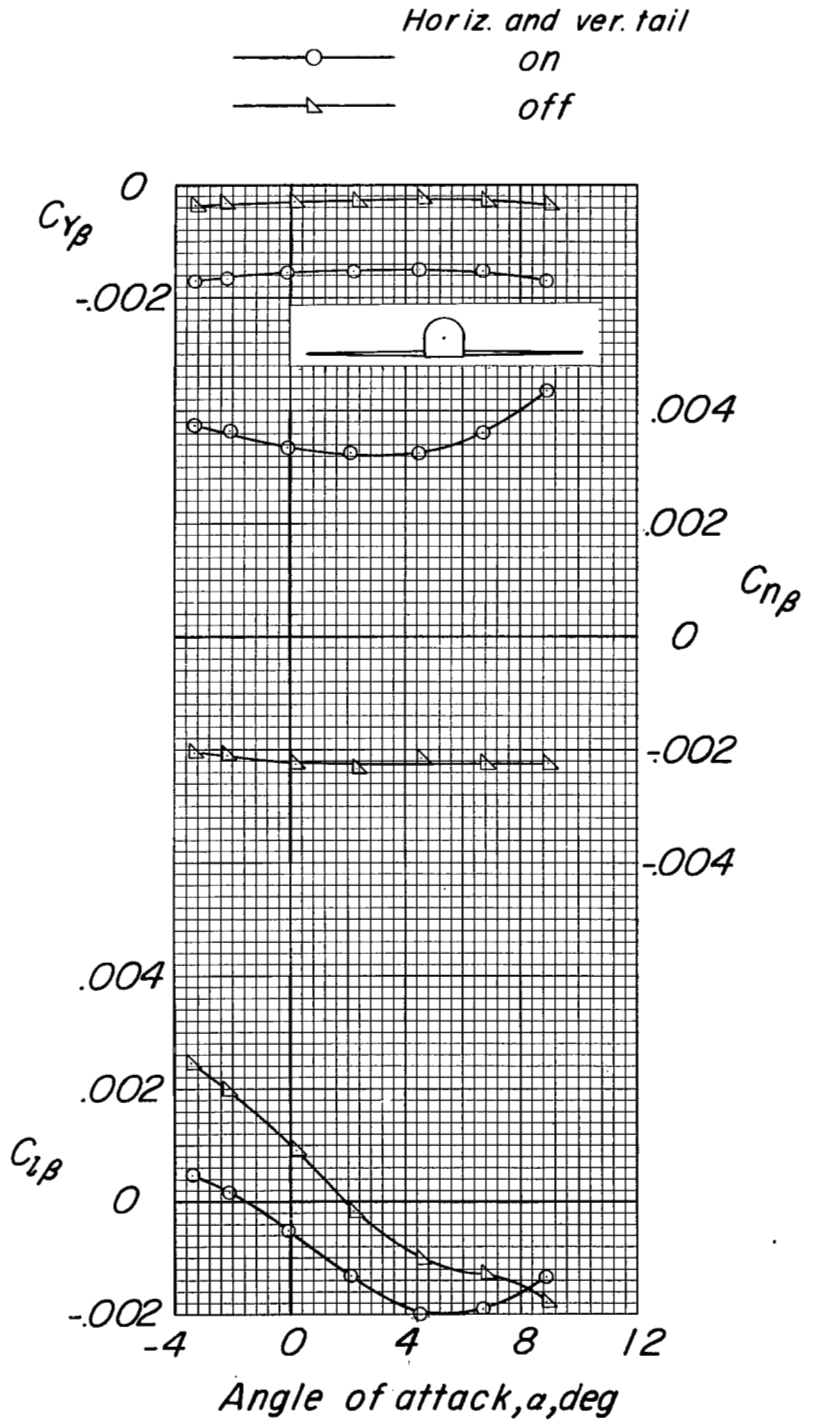

(d) M = 0.92.

Figure 13.- Concluded.

[redacted]

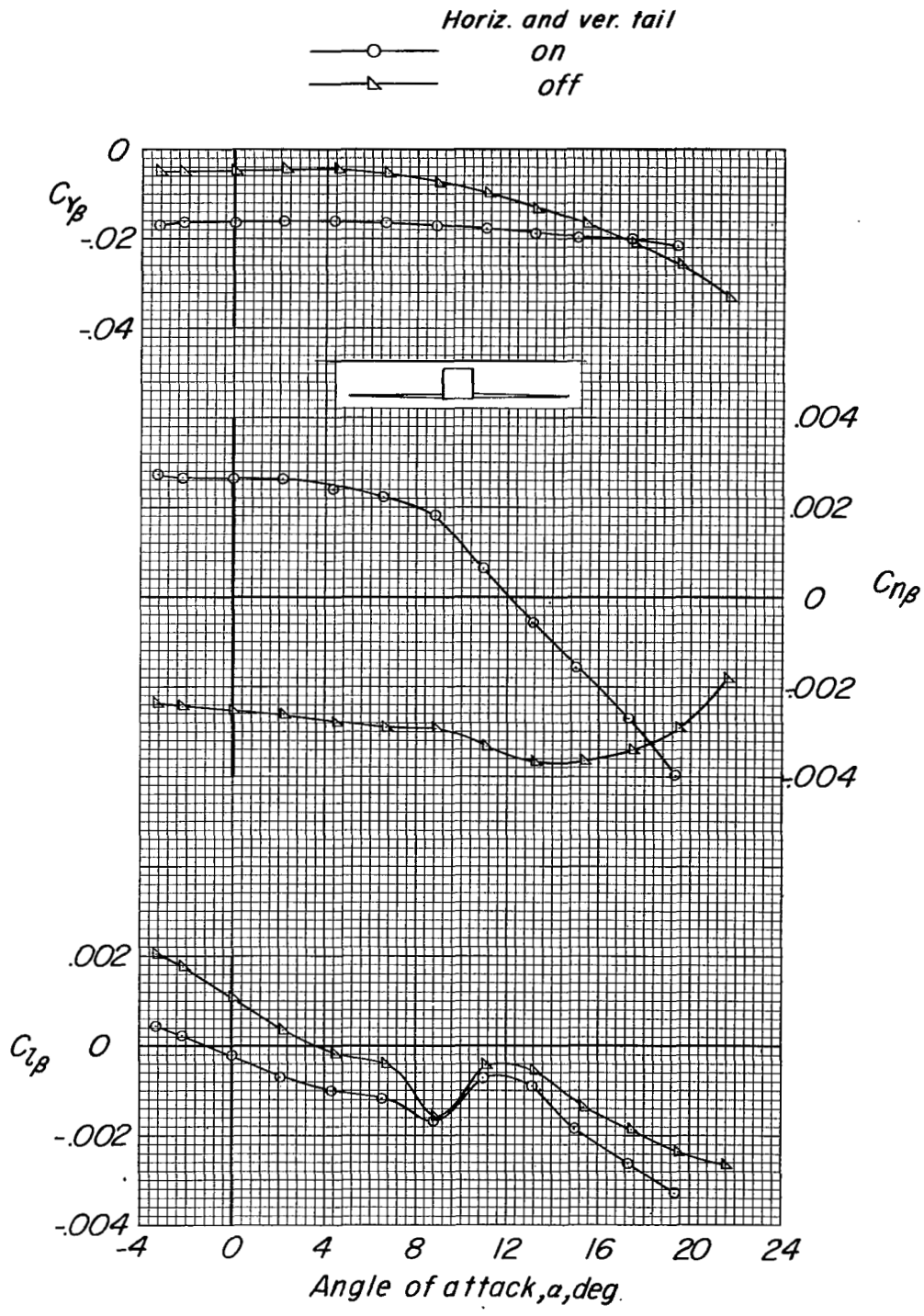

(a) M = 0.80.

Figure 14.- Lateral stability parameter characteristics of model with low wing and square fuselage.

[redacted]

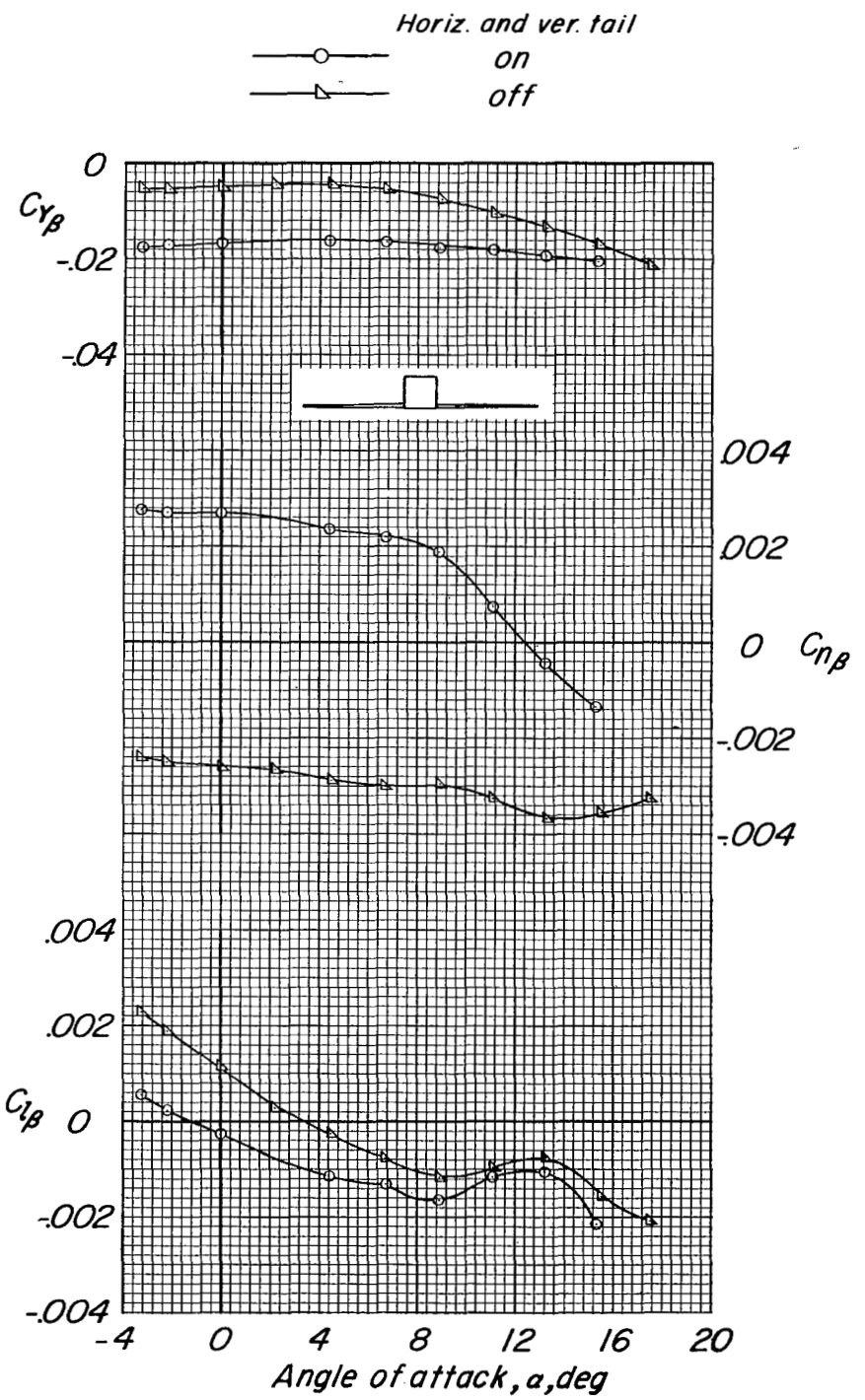

(b) M = 0.85.

Figure 14.- Continued.

[redacted]

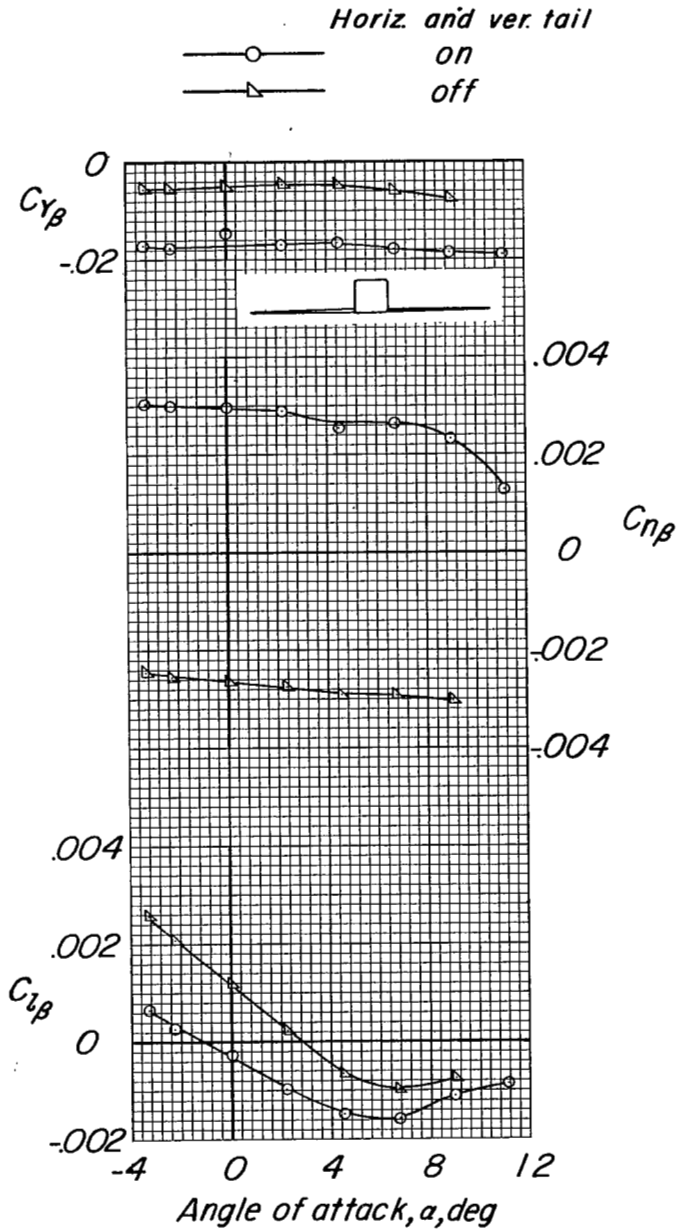

(c) M = 0.90.

Figure 14.- Continued.

[redacted]

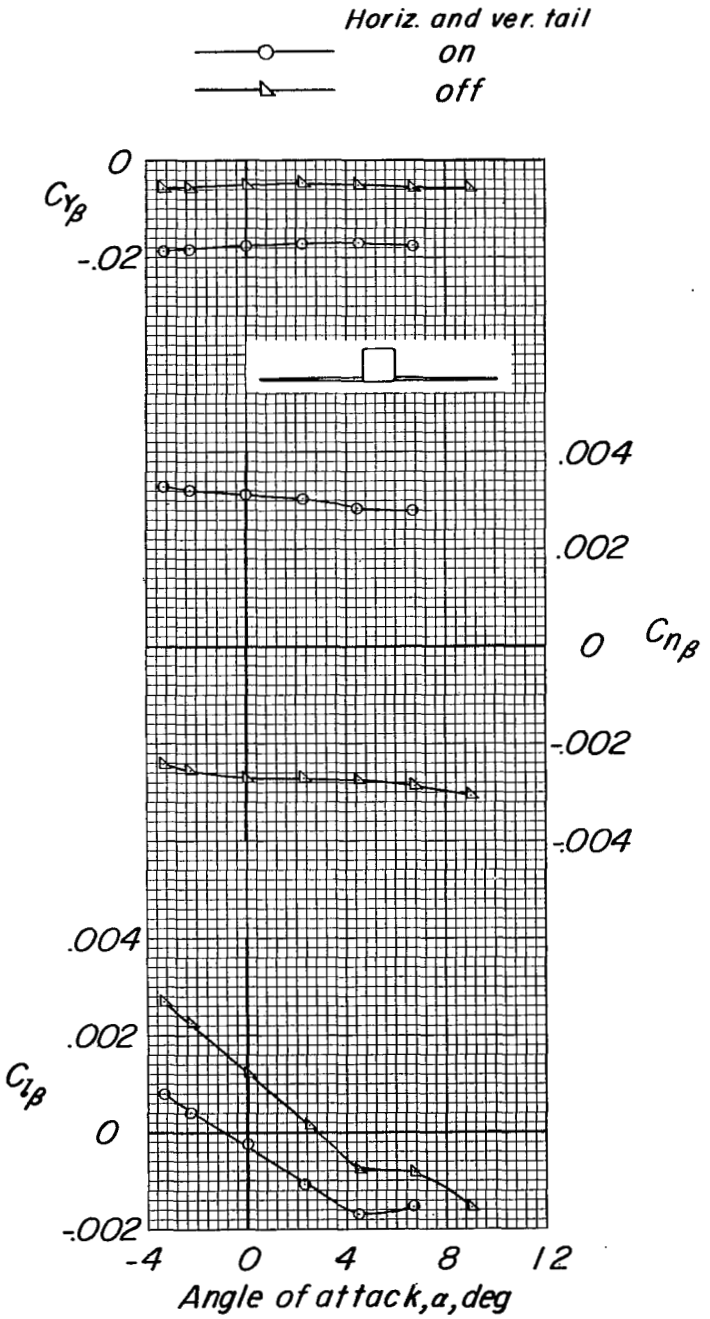

(d) M = 0.92.

Figure 14.- Concluded.

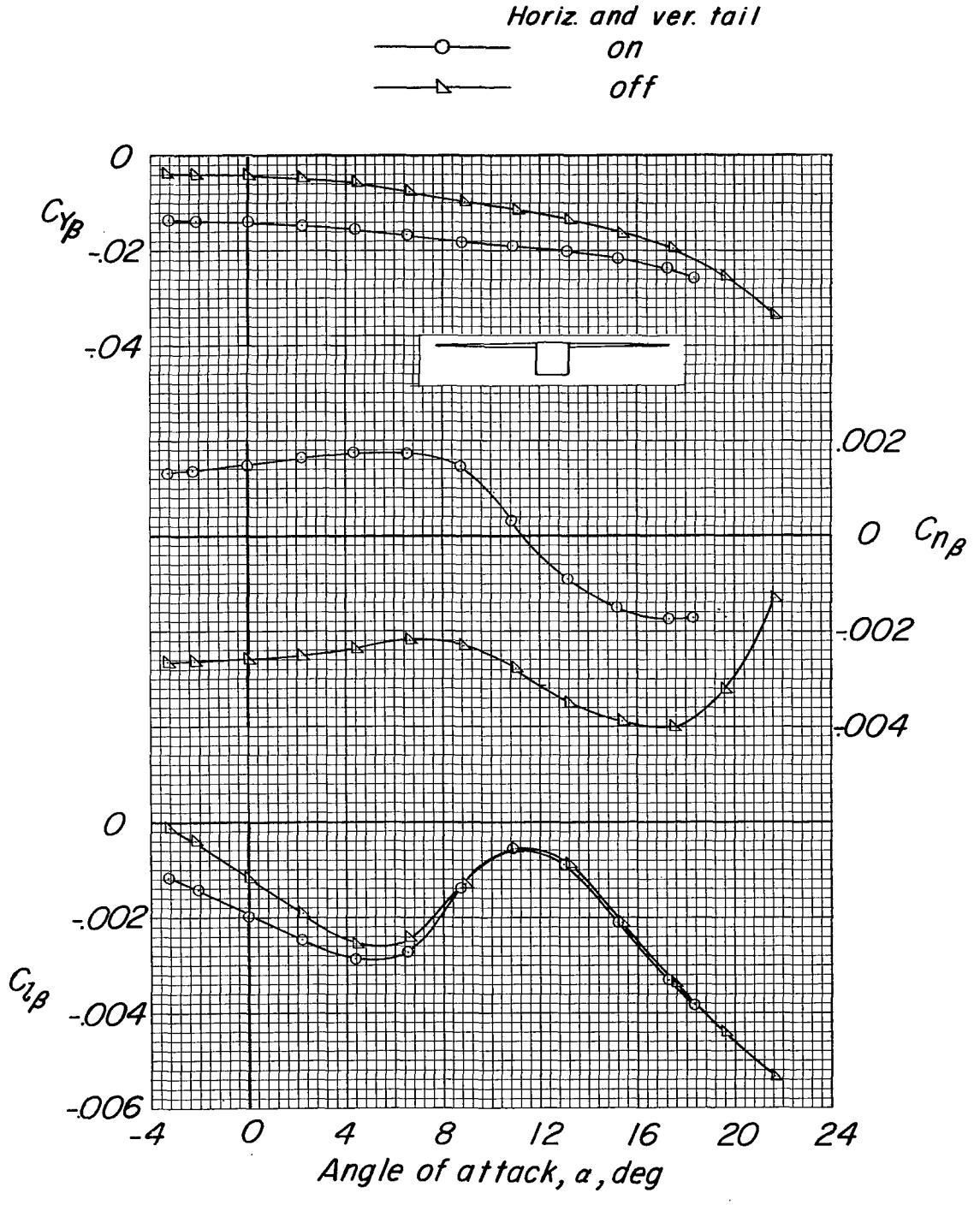

(a) M = 0.80.

Figure 15.- Lateral stability parameter characteristics of model with high wing and square fuselage.

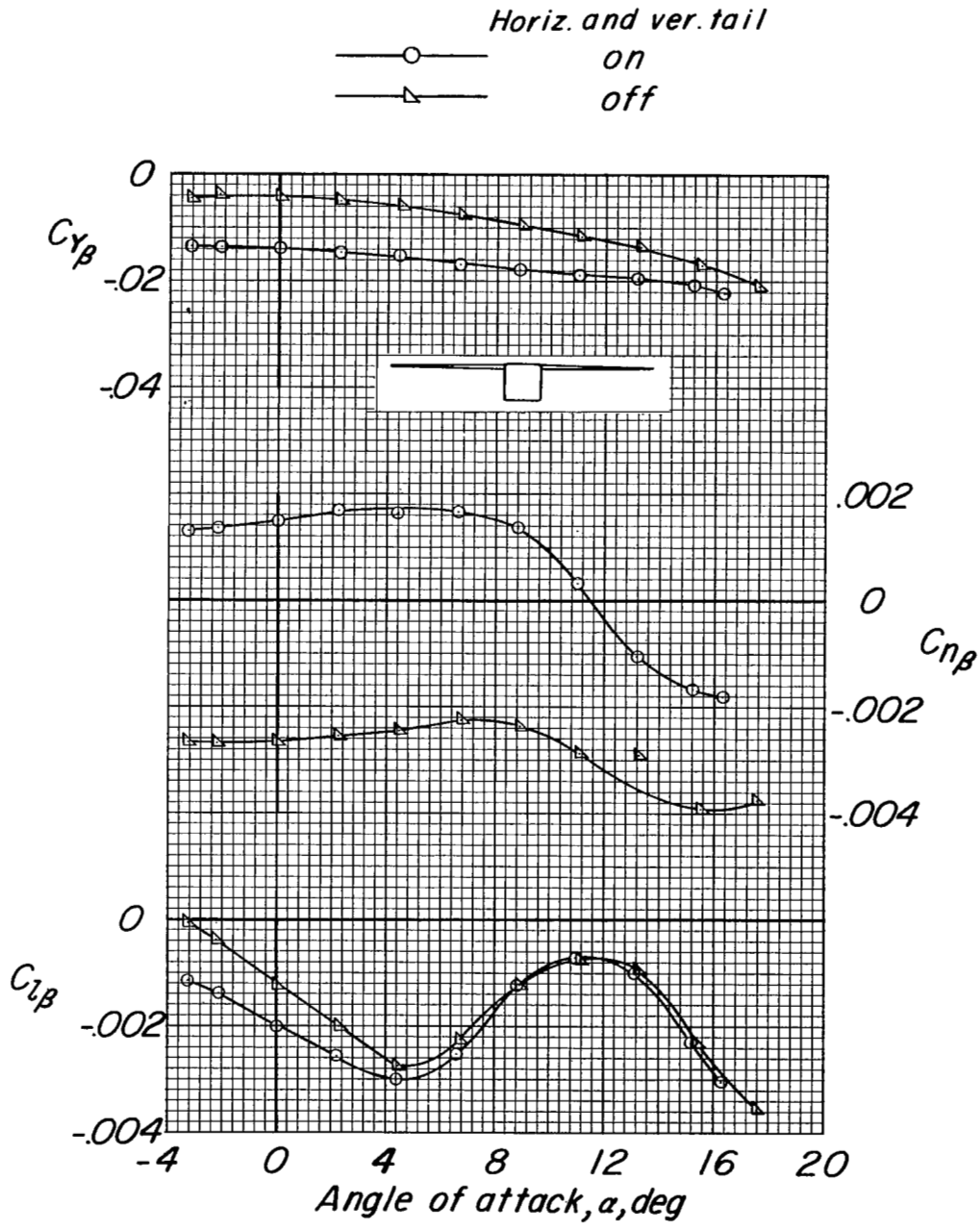

(b) M = 0.85.

Figure 15.- Continued.

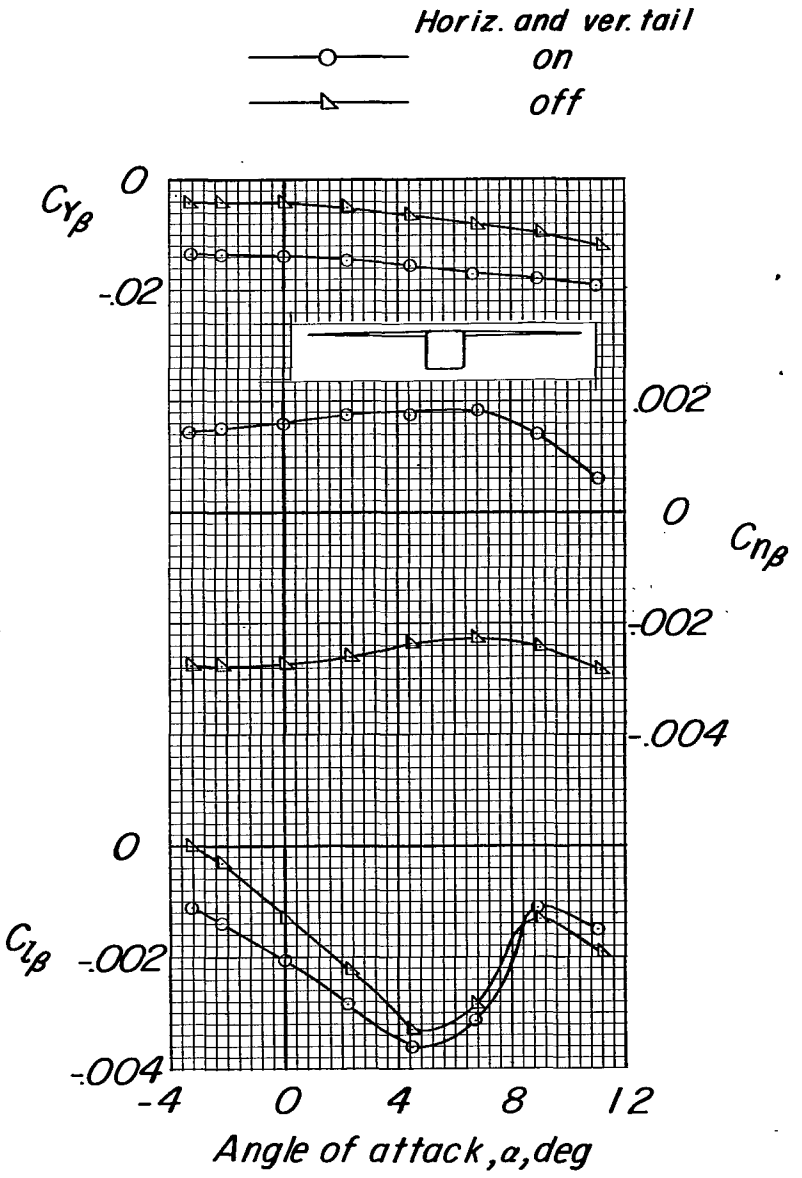

(c) M = 0.90.

Figure 15.- Continued.

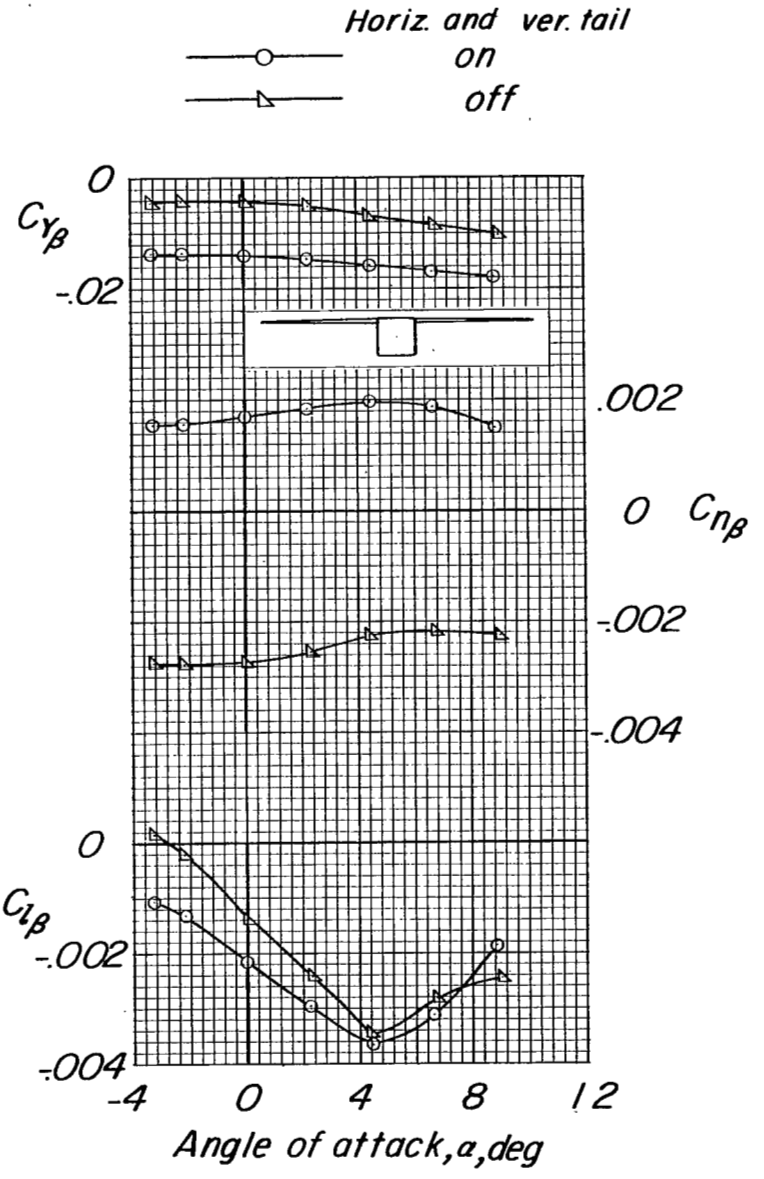

(d) M = 0.92.

Figure 15.- Concluded.

[redacted]

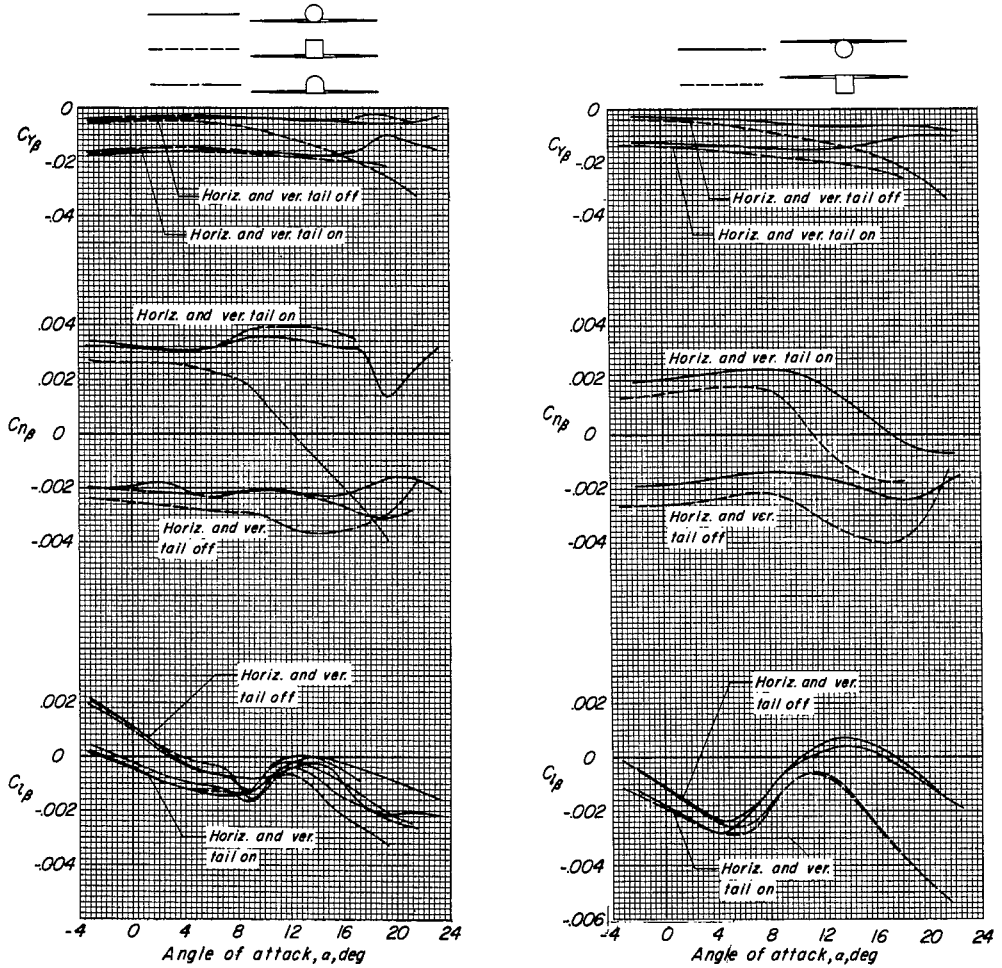

Figure 16.- Comparison of variation of static lateral stability derivatives with angle of attack of circular, square, and half-circular-half-square cross-section fuselage models. M = 0.80.

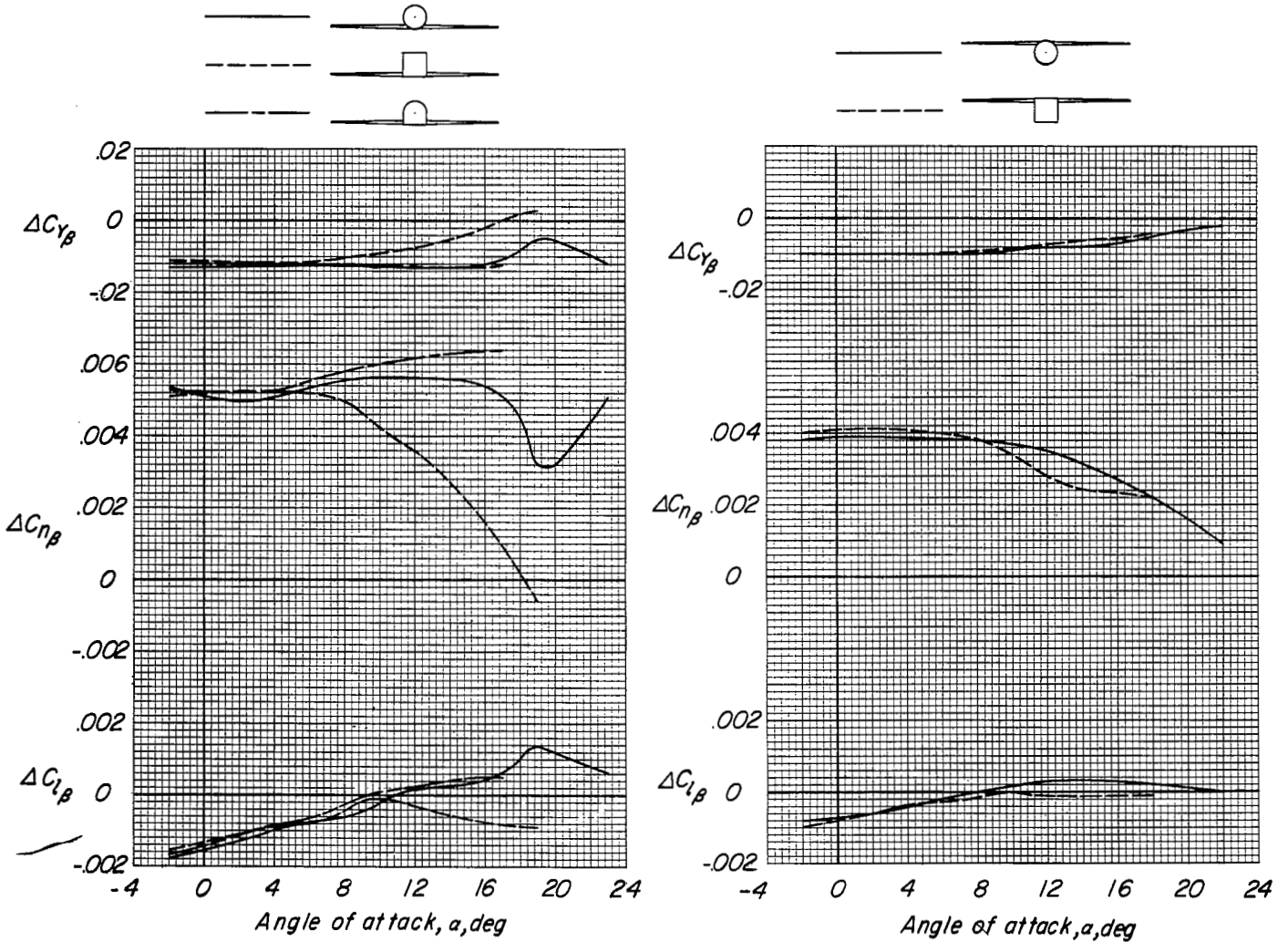

Figure 17.- Variation with angle of attack of the increments of the static lateral derivatives due to the tail. M = 0.80.